



REVIEW

Characteristic roadmap of linker governs the rational design of PROTACs



Yawen Dong^a, Tingting Ma^a, Ting Xu^a, Zhangyan Feng^a, Yonggui Li^a,
Lingling Song^a, Xaojun Yao^{c*}, Charles R. Ashby Jr^{d*}, Ge-Fei Hao^{b*}

^aSchool of Pharmaceutical Sciences, Guizhou University, Guiyang 550025, China

^bState Key Laboratory of Green Pesticide, Key Laboratory of Green Pesticide and Agricultural Bioengineering, Ministry of Education, Center for R&D of Fine Chemicals, Guizhou University, Guiyang 550025, China

^cFaculty of Applied Sciences, Macau Polytechnic University, Macau 999078, China

^dDepartment of Pharmaceutical Sciences, St. John's University, New York, NY 11439, USA

Received 6 February 2024; received in revised form 11 February 2024; accepted 2 April 2024

KEY WORDS

PROTAC;
PROTAC linker;
Linker characteristics;
Rational design;
Biodegradation efficiency

Abstract Proteolysis targeting chimera (PROTAC) technology represents a groundbreaking development in drug discovery, leveraging the ubiquitin–proteasome system to specifically degrade proteins responsible for the disease. PROTAC is characterized by its unique heterobifunctional structure, which comprises two functional domains connected by a linker. The linker plays a pivotal role in determining PROTAC's biodegradative efficacy. Advanced and rationally designed functional linkers for PROTAC are under development. Nonetheless, the correlation between linker characteristics and PROTAC efficacy remains under-investigated. Consequently, this study will present a multidisciplinary analysis of PROTAC linkers and their impact on efficacy, thereby guiding the rational design of linkers. We will primarily discuss the structural types and characteristics of PROTAC linkers, and the optimization strategies used for their rational design. Furthermore, we will discuss how factors like linker length, group type, flexibility, and linkage site affect the biodegradation efficiency of PROTACs. We believe that this work will contribute towards the advancement of rational linker design in the PROTAC research area.

© 2024 The Authors. Published by Elsevier B.V. on behalf of Chinese Pharmaceutical Association and Institute of Materia Medica, Chinese Academy of Medical Sciences. This is an open access article under the CC BY-NC-ND license (<http://creativecommons.org/licenses/by-nc-nd/4.0/>).

*Corresponding authors.

E-mail addresses: xjyao@mpu.edu.mo (Xiaojun Yao), cnsratdoc@optonline.net (Charles R. Ashby), gefei_hao@foxmail.com (Ge-Fei Hao).
Peer review under the responsibility of Chinese Pharmaceutical Association and Institute of Materia Medica, Chinese Academy of Medical Sciences.

1. Introduction

The proteolysis targeting chimeras (PROTACs) hold remarkable promise for resolving issues related to small-molecule inhibitors^{1–4}. These inhibitors frequently encounter difficulties in targeting proteins that are considered “undruggable”, are more likely to develop resistance, and often necessitate higher systemic drug concentrations to maintain therapeutic efficacy^{5–8}. As a novel drug development approach, PROTACs use the UPS (ubiquitin–proteasome system) to biodegrade specific proteins, thereby increasing the probability of successfully overcoming these challenges^{7,9–11}. This process occurs by a catalytic mechanism that leads to the dissociation of the target protein following polyubiquitination, producing therapeutic efficacy at lower concentrations¹². PROTACs biodegrade target proteins of various conformations, which can overcome drug resistance due to target mutations, produce an increase in the durations of action, minimize off-target effects, and decrease the incidence of adverse effects. Furthermore, inactive or less active inhibitors can be converted into potent biodegraders^{13,14}. As a result of these beneficial characteristics, PROTAC has garnered significant interest from both academic and industrial researchers, leading to a significant increase in the number of published studies on PROTAC¹⁵.

PROTAC is a unique molecule that has heterobifunctionality, characterized by a linker component that effectively links a protein of interest (POI) ligand with an E3 ubiquitin ligase (E3) recruiting ligand¹⁶. The unique configuration of PROTAC facilitates the establishment of a stable ternary complex between E3 ligase and POI. This ternary complex produces the selective polyubiquitination of the POI, ultimately leading to its biodegradation by the UPS (Fig. 1)¹⁷. Numerous studies have reported the crucial role of the linker in determining the efficacy of PROTAC¹⁸. The linker not only supports the stable formation of the ternary complex but also affects the physicochemical and pharmacokinetic properties of PROTACs^{19,20}. The length, group type, flexibility, and linkage site of the linker all impact the stability of the ternary complex and, ultimately, the biodegradation efficiency of PROTACs^{21,22}. Given these intricate relationships, it is evident

that the linker is the essential factor in ensuring greater specificity and targeting efficiency of PROTACs²³.

Recently, there has been a growing number of publications reporting progress in the design and optimization of PROTAC linkers. These efforts have primarily focused on linker length, group type, flexibility, and linkage site. For instance, Wurz et al.²⁴ discovered that increasing the linker length facilitated the formation of a ternary complex, ultimately increasing the biodegradation efficiency of PROTAC for the protein, bromodomain and extraterminal domain-4 (BRD4). Similarly, Han et al. replaced an alkyl chain with a pyridyl group of similar length, creating a potent PROTAC for the biodegradation of the androgen receptor (AR), by increasing solubility and pharmacokinetics²⁵. Farnaby et al. increased linker rigidity by introducing a phenyl group, leading to an additional T-shaped stacking interaction that increased the potency of the PROTAC for (BAF)/phospho-BAF chromatin remodeling complexes²⁶. Zengerle et al. used crystallographic data to identify an optimal linkage site that would increase the protein–protein interactions, directly increasing the PROTAC’s efficacy for BRD4²⁷. These studies have significantly advanced the PROTAC field and provided valuable insights for the design of linkers. However, there is still a need for more advanced and well-designed functional linkers to further revolutionize PROTAC technology²³. To date, the relationship between linker characteristics and PROTAC efficacy has rarely been systematically explored.

In this study, we have focused our efforts on the multidisciplinary analysis of the structures and properties of PROTAC linkers and their effect on the biodegradation efficacy of PROTACs. Our major objective is to offer valuable insights into the rational design of PROTAC linkers. We have primarily examined three key areas: 1) an analysis of the various structural types and characteristics of PROTAC linkers reported to date; 2) the optimization strategies utilized in the rational design of effective PROTAC linkers; and 3) the impact of linker length, group type, flexibility, and linkage site on the ternary complex formation, pharmacokinetics, protein–protein interactions, and ultimately, PROTAC biodegradation efficiency. We use case studies to demonstrate these comprehensive effects. We hope that

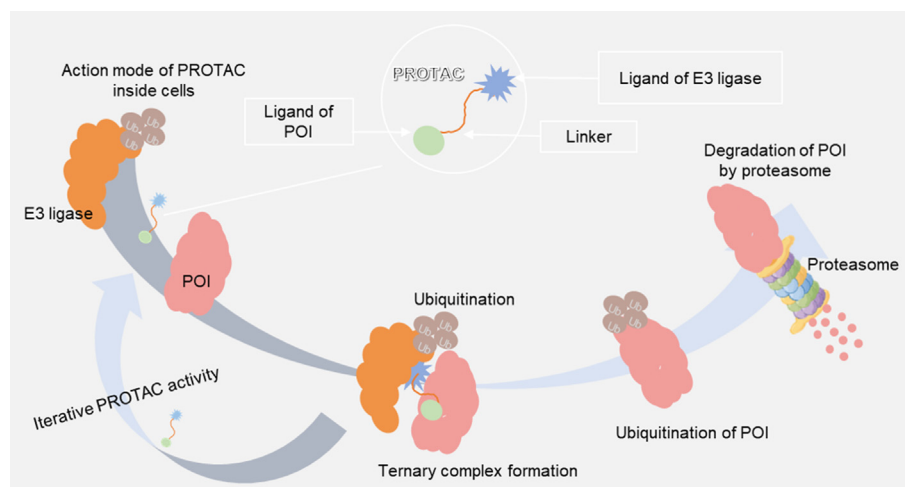


Figure 1 The three key components of PROTAC are: 1) the E3 ligase ligand; 2) the POI ligand and 3) the linker connecting the two ligands. The PROTAC’s mode of action within cells involves promoting the interaction among the POI and E3 to produce a stable ternary complex. POI is ubiquitinated as a result of this interaction and subsequently biodegraded by proteasomes, which typically consume multiple ubiquitin molecules labeled with the POI.

our work will increase the understanding of PROTAC linker rational design, thereby facilitating future research in this field.

2. Structural types and characteristics of PROTAC linkers

2.1. An overview of existing PROTAC linkers

Given the crucial role of the linkers in PROTACs, we carried out a thorough examination of the various linker structural types and their frequencies in reported PROTACs, spanning from the first reported PROTAC in 2001²⁸ to the end of 2023. Based on a statistical principle, we only selected the linker of the most potent PROTAC in each paper for analysis. Our dataset comprises a total of 337 PROTACs. By analyzing the linkers of these PROTACs, we found that they can be categorized into two broad groups, according to their structural types: flexible linkers and relatively rigid linkers. The flexible linkers are the most widely used type, accounting for 67.66% of the total. These mainly include alkyl-based linkers and polyethyleneglycol-based (PEG-based) linkers, which account for 44.81% and 22.85% of the total, respectively (Fig. 2A). The flexible linkers are considered a standard feature in the PROTAC field, and they can not only enable systematic variations in linker length but also facilitate the rapid synthesis of molecules with distinct linkers^{29–34}. The relatively rigid linkers account for 32.34% of the total and encompass eight types. Among them, triazole-based linkers and cycloalkane-based linkers are the two most commonly used types, accounting for 12.17% and 12.76% of the total, respectively. The advent of “click chemistry” reaction^{24,35,36}, allows for the insertion of triazole-based linkers into PROTACs, which significantly addressed the challenges of synthesis in this field, thereby increasing the utilization rate of these linkers³⁷. The cycloalkane-based linkers, particularly piperazine and piperazine groups, are the most widely used due to their excellent stability and chemical reactivity. These properties allow for the modulation of PROTAC polarity, thereby meeting design requirements and increasing cell permeability and biodegradation efficacy^{38–40}. Additionally, in the relatively rigid linkers, the optically controlled linkers have increasingly been used as linkers in recent years^{41–46}. These linkers introduce light-responsive protective groups, yielding PROTACs with increased targeting specificity, greater stability, and unique on-off interactions. This linker type holds significant promise in the field of PROTACs and will likely be widely used due to its potential in cancer precision diagnosis⁴⁴. Overall, our analysis highlights the large diversity of linker structures and emphasizes the need for the design of novel linkers to increase PROTAC biodegradability.

To understand the emergence of different linker types over time, we examined the timeline in Fig. 2B. The initial linker introduced in 2001 was a flexible linear alkyl chain, which was utilized in the first PROTAC design²⁸. In 2008, the amphiphilic PEG chain was introduced to enhance solubility and cell permeability⁴⁷. In contrast, a fused heterocycle-based linker, the first relatively rigid linker, emerged in 2016 through bio-orthogonal click chemistry⁴⁸. This was followed by a notable increase in PROTAC-related publications, highlighting their growing popularity and significance. Since 2018, additional linker types have been introduced, including the aromatic⁴⁹ and triazole-based linkers^{24,40,50–54}. In 2019, cycloalkane^{25,55–57}, spiro^{58,59}, photo-caged⁴⁵ and photo-switchable-based linkers^{41–46}, were introduced. In 2020, a macrocyclic-based linker was designed, using computational

modeling to produce the most potent PROTACs⁶⁰. The significant growth in PROTAC linker diversity can be attributed to advancements in synthesis technology and more rational design strategies. These advancements will further facilitate the development of the PROTAC field^{19,24,61–66}.

2.2. Flexible linkers

Flexible linkers, chains of a certain length that may be saturated or unsaturated⁶⁷, are often categorized as alkyl-based or PEG-based linkers depending on their structural features (Table 1)^{13,68–70}. These linkers are standard in the PROTAC field. The alkyl-based linker, which is based on saturated or unsaturated alkyl chains, often contains oxygen, nitrogen, carbonyl, secondary amine, or an amide, inserted at various locations^{30,71–74}. This linker is highly stable under physiological conditions and has a simple structure, making it relatively easy to synthesize³⁰. It effectively links the warhead and the E3 ligase binder. However, this linker is frequently hydrophobic, leading to the poor water solubility of the resulting PROTAC and affecting its properties in physiological environments^{68,75}. In fact, introducing polar groups into the structure can solve this problem, and these polar groups can also be used for further modification and connection with other groups^{68,75}. Furthermore, these linkers are more susceptible to oxidative metabolism *in vivo*. For example, Khan et al.⁷⁶ discovered a selective BCL-X_L PROTAC degrader DT2216, with an aliphatic linker, to achieve safe and potent antitumor efficacy. The linker adds flexibility to DT2216 and its optimal length allows for the introduction of the favorable formation of a BCL-X_L-DT2216-VHL ternary complex, resulting in greater BCL-X_L biodegradation efficacy. Additional examples are presented in Table 1 and Supporting Information Table S1.

In alkyl-based linkers, various amino acids or short peptide sequences, such as amino hexanoic acid (Ahx), glycine, serine, and GSGS, are used as linkers in peptide PROTACs^{12,77,78}. Although these PROTACs have produced effective biodegradation of numerous targets, they often have limited cell permeability and are highly susceptible to cleavage by proteases. To address these limitations, amino acids or short peptide sequences with cell-penetrating capabilities have been introduced to increase flexibility and facilitate the uptake of the PROTACs into intact cells⁷⁹. The GSGS linker is currently the most widely used. This linker, along with the resulting PROTAC, can be easily synthesized using the standard Fmoc method. Lu et al.¹² have developed a Keap1-dependent peptide PROTAC that degrades tau protein by the UPS degradation pathway. This PROTAC uses a short GSGS peptide to link the tau recognition moiety to the Keap1 binding moiety, increasing its flexibility and binding capabilities. Other examples are provided in Table 1 and Table S1.

The PEG-based linkers often consist of two or more consecutive ethylene glycol units and can be integrated with other chains (Table 1)^{26,80–83}. PEG's hydrophilic nature increases the water solubility of PROTACs, increasing their adaptability to physiological environments³⁰. PEG's capacity to attach multiple chemical functions enhances the modifiability of PROTACs and their connectivity to other groups⁸⁴. Furthermore, PEG has good compatibility *in vivo*, mitigating the risk of inducing an immune response or toxicity⁶¹. Nevertheless, compared to alkyl-based linkers, PEG-based linkers may have reduced stability under specific physiological conditions and their synthesis can be more complicated. The significant cost of PEG's raw materials can also

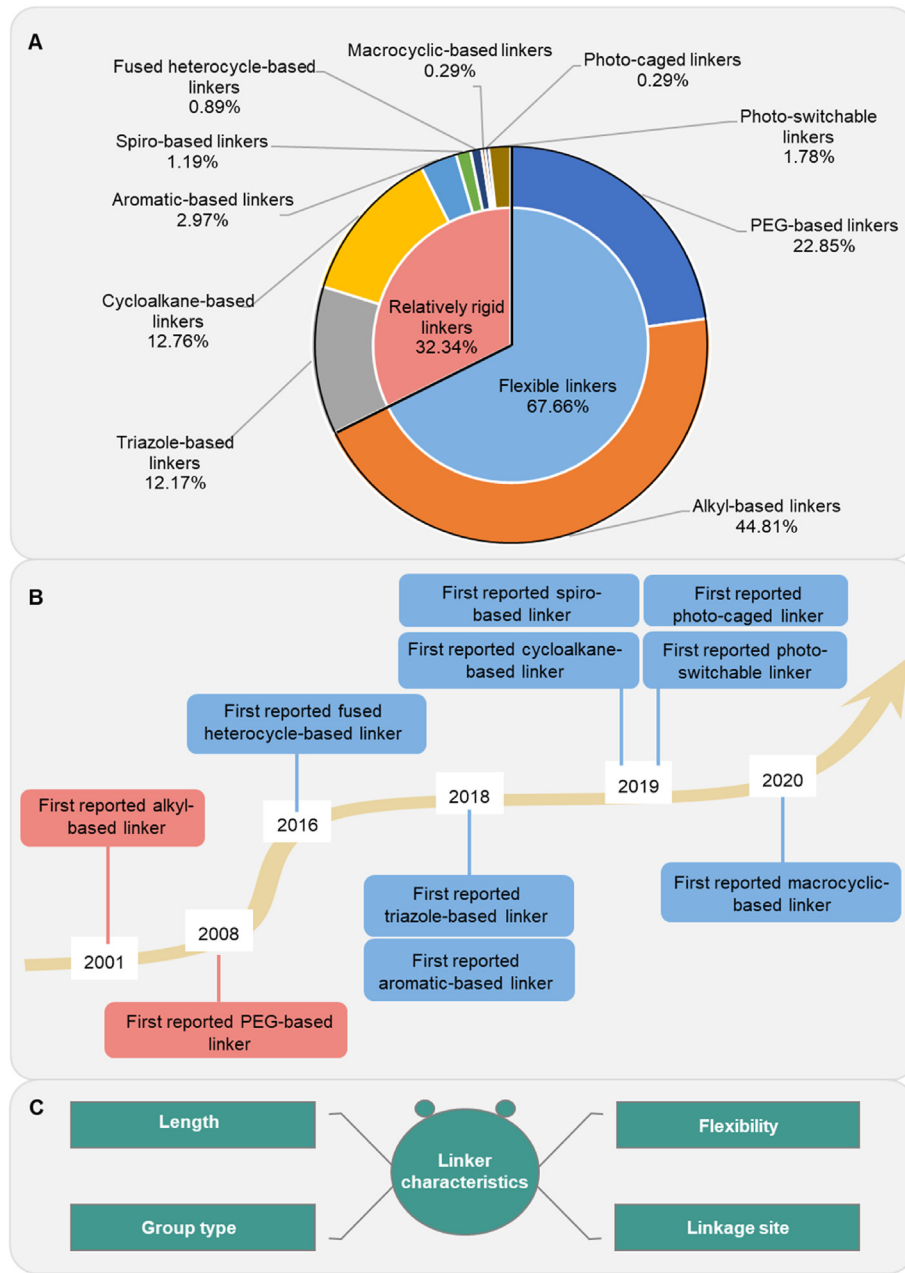


Figure 2 Structural types and characteristics of PROTAC linkers. (A) The frequency of occurrence of each type of linker in PROTACs encompasses the period from the initial report of PROTAC in 2001 up until the end of 2023. We have only counted the linker in the most effective PROTAC described in each publication. (B) A timeline has been created to indicate the initial appearance of each linker type in the scientific literature. (C) The linker characteristics that impact the biodegradation efficiency of the PROTAC have been identified.

contribute to an increase in the overall cost of PROTACs. Furthermore, these linkers are more susceptible to oxidative metabolism *in vivo*. For example, Crews et al.⁸⁵ used a PEG linker to conjugate a classic BRD4 binding motif from the triazolo-diazepine acetamide with a cereblon (CRBN) binding motif from the IMiD class pomalidomide, resulting in the potent PROTAC ARV-825, which has anticancer efficacy. The PEG linker's significant conformational flexibility optimized the ternary complex establishment between PROTAC, BRD4, and CRBN, thus producing an efficacious compound. Additional information is provided in Table 1 and Table S1.

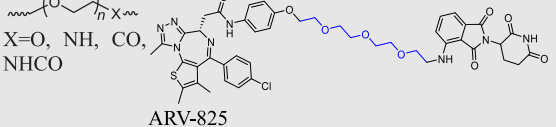
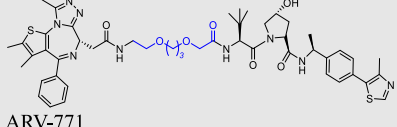
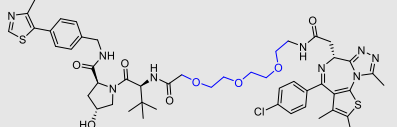
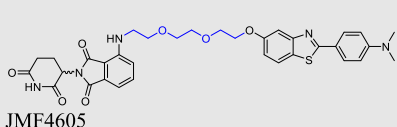
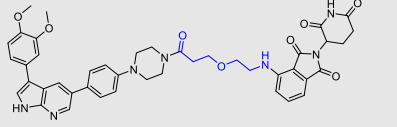
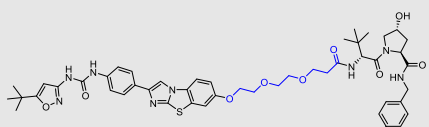
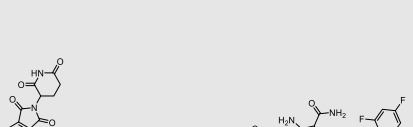
2.3. Relatively rigid linkers

The linkers containing cyclic structures have been characterized as being relatively rigid^{40,48,86,87}. Depending on the type of cyclic structures, these linkers can be further categorized into several types, including triazole⁸⁷, aromatic⁸⁸, cycloalkane⁵⁵, spiro⁵⁹, fused heterocycle³², and macrocyclic-based⁶⁰. Table 1 provides a comprehensive list of these types of cyclic structures. The triazole- and cycloalkane-based linkers are the most widely used. Triazole-based linkers contain a triazole group, which is easily accessible through copper-catalyzed azide–alkyne cycloaddition

Table 1 The types of PROTAC linkers and their associated information.

Linker type	Common structure	Representative PROTAC	POI	E3 ligase	Ref.
Flexible linker	Alkyl-based linker 	 DT2216	BCL-X _L	VHL	76
	X=O, NH, CO, NHCO,	 dBET1	BET	CRBN	32
		 dBET6	BET	CRBN	107
		 FM-74-103	GSPT1	CRBN	108
		 ITRI-90	AR	VHL	109
		 DD-2	PLK1	VHL	110
		 ZZ151	SOS1	VHL	111
		 KH103	GR	CRBN	112

Table 1 (continued)

Linker type	Common structure	Representative PROTAC	POI	E3 ligase	Ref.
		YQQYQDATAEQG ~GSGS~LDPETGEYL-(D-R) ₈ Peptide 1	Tau	Keap1	12
			ERα	VHL	77
PEG-based linker	X=O, NH, CO, NHCO		BRD4	CRBN	85
			BET	VHL	33
			BRD4	VHL	27
			TDP-43	CRBN	113
			HPK1	CRBN	114
			FLT-3	VHL	13
			BTK	CRBN	6

(continued on next page)

Table 1 (continued)

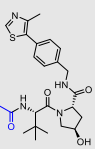
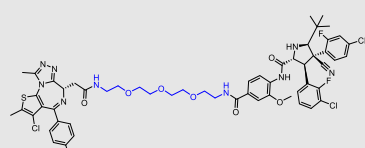
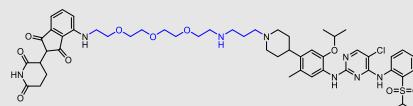
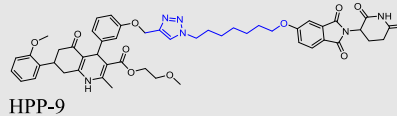
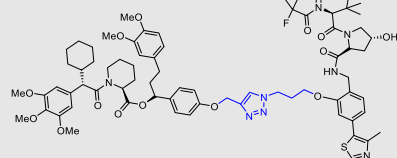
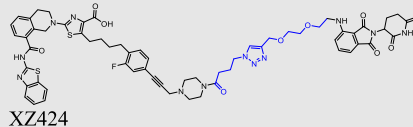
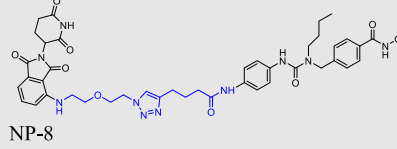
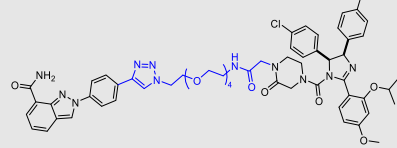
Linker type	Common structure	Representative PROTAC	POI	E3 ligase	Ref.
			FAK	VHL	115
			BRD4, P53	MDM2	21
			ALK	CRBN	116
Relatively rigid linker	Triazole-based linker		BRD3, BRD4	CRBN	117
			FKBP51	VHL	118
			BCL-X _L	CRBN	103
			HDAC6	CRBN	119
			PARP1	MDM2	38

Table 1 (continued)

Linker type	Common structure	Representative PROTAC	POI	E3 ligase	Ref.
			FAK	CRBN	120
			p38	CRBN	121
			ER	cIAP1	122
			Sirt2	CRBN	51
			MAFF	cIAP1	123
Cycloalkane-based linker			AR	CRBN	98
		ER	CRBN	97
			SHP2	VHL	124

(continued on next page)

Table 1 (continued)

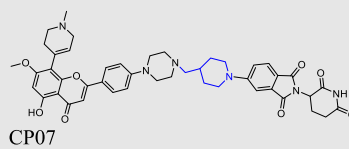
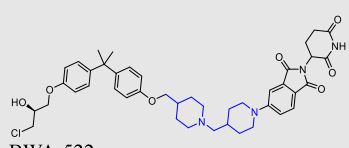
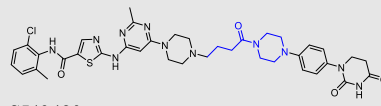
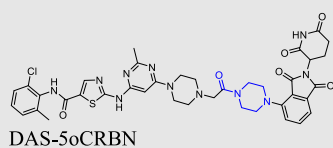
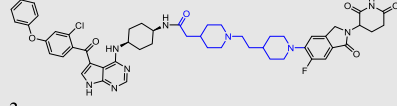
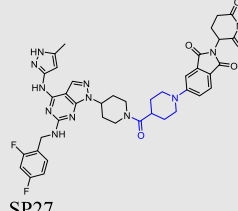
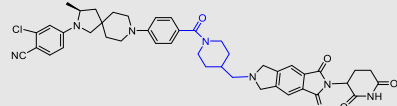
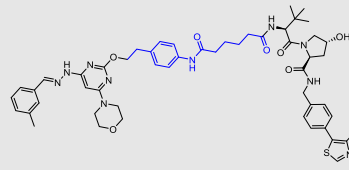
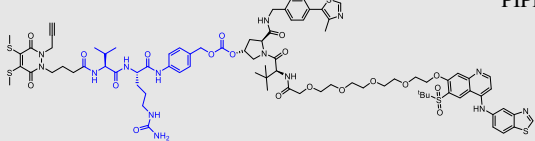
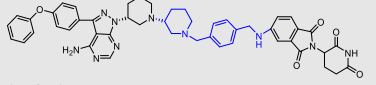
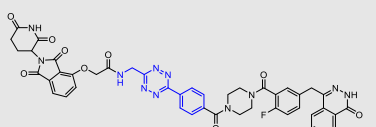
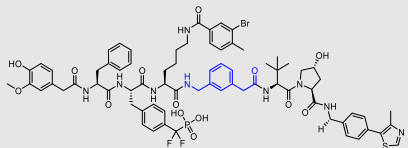
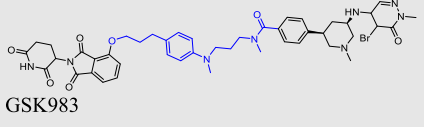
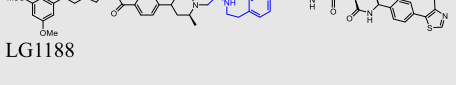
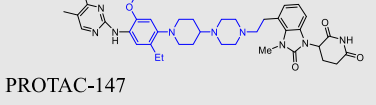
Linker type	Common structure	Representative PROTAC	POI	E3 ligase	Ref.
			CDK9	CRBN	125
			AR	CRBN	126
			LCK	CRBN	127
			c-Src	CRBN	128
			BTK	CRBN	129
			PLK4	CRBN	130
			AR	CRBN	131
Aromatic-based linker			PIKfyve	VHL	106

Table 1 (continued)

Linker type	Common structure	Representative PROTAC	POI	E3 ligase	Ref.
			PIPK2	VHL	132
			BTK	CRBN	133
			BET	CRBN	134
			PTP1B, TC-	CRBN PTP	90
			PCAF, GCN5	CRBN	49
			AR	VHL	135
			FGFR1	VHL	136
			EGFR	CRBN	137

(continued on next page)

Table 1 (continued)

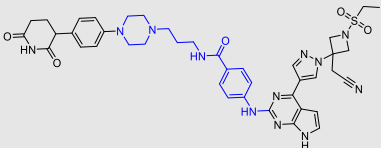
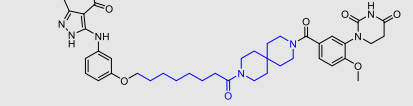
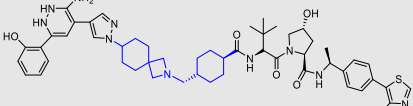
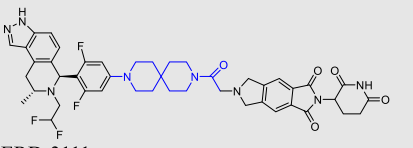
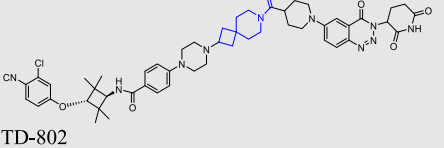
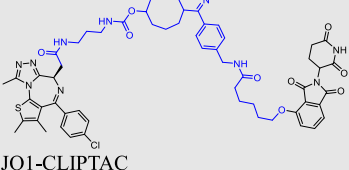
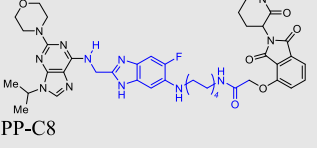
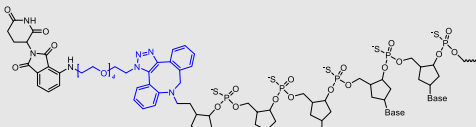
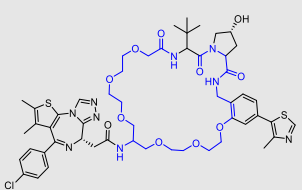
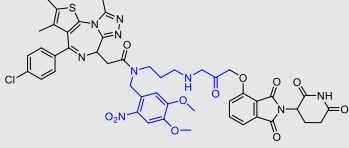
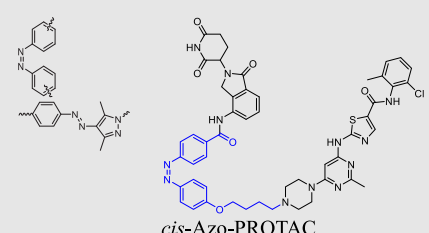
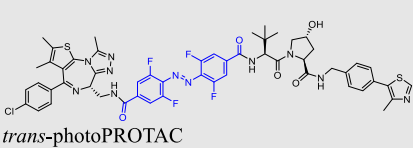
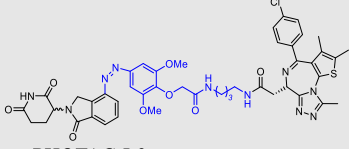
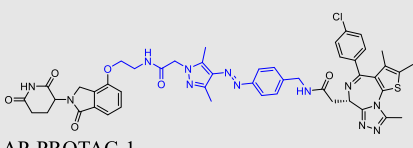
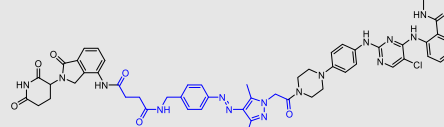
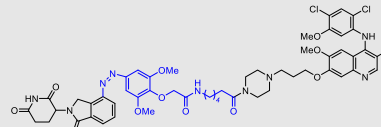
Linker type	Common structure	Representative PROTAC	POI	E3 ligase	Ref.
			GSPT1	CRBN	138
Spiro-based linker			MLKL	CRBN	139
			SMARCA2	VHL	140
			ERα	CRBN	141
			AR	CRBN	58
Fused heterocycle-based linkers			BRD4	CRBN	48
			CDK12	CRBN	102

Table 1 (continued)

Linker type	Common structure	Representative PROTAC	POI	E3 ligase	Ref.
			NSPs	CRBN	93
PS-ApTCS					
Macrocyclic-based linker	—		BRD4	VHL	60
Photo-caged linkers			BRD4	CRBN	45
Photo-switchable linkers			BCR-ABL	CRBN	41
			BRD2, BRD4	VHL	43
			BRD2, BRD3, BRD4, FKBP12	CRBN	44
			BRD2, BRD4	CRBN	46

(continued on next page)

Table 1 (continued)

Linker type	Common structure	Representative PROTAC	POI	E3 ligase	Ref.
		 <p>AP-PROTAC-2</p>	FAK, AURORA-A, TBK1	CRBN	46
		 <p>cis-CAMKIIα-PROTAC</p>	CaMKIIα	CRBN	42

(CuAAC) reaction, also known as “click chemistry”⁸⁹. The click reaction efficiently produces the triazole moiety with near-stoichiometric yield under mild conditions. This reaction has excellent compatibility with other functional groups, even in the presence of water⁹⁰. This has greatly facilitated the application of this type of linker in the PROTAC field⁹¹. Furthermore, unlike the flexible linkers, which are more prone to oxidative metabolism *in vivo*, the triazole structure is more stable *in vivo* and has a longer duration of action⁹². As an example, Bagka et al. have developed a long-acting Hedgehog pathway inhibitor, PROTAC HPP-9, which utilizes a triazole-based linker to prolong biodegradation of BET bromodomains. The rigid linker in this compound ensures a stable interaction between the warhead HPI-1 and the POI, whereas the optimal linker length allows both moieties bind to their respective proteins, forming a stable low-energy complex⁹³. Other examples are summarized in Table 1 and Table S1.

The cycloalkane-based linkers, a commonly utilized class of rigid linkers, frequently incorporate fragments of piperazine⁹⁴, piperidine⁵⁵, tetrahydropyrrole⁹⁵, or cyclohexane⁹⁶. Currently, the inclusion of piperazine and piperidine fragments is particularly prevalent. These linkers increase the metabolic stability of the resulting PROTACs, producing a longer duration of action, while maintaining their structural integrity⁹⁴. Furthermore, they increase the water solubility of PROTACs, facilitating their dissolution and distribution within the body⁶⁰. Currently, multiple PROTACs containing this type of linker are undergoing evaluation in clinical trials: ARV-471⁹⁷, ARV-110⁹⁸, CFT8634⁹⁹, KT-413¹⁰⁰, and NX2127¹⁰¹. ARV-110 is a pertinent example. It selectively targets and produces the biodegradation of the androgen receptor (AR) protein, and is being developed to treat metastatic castration-resistance prostate cancer (mCRPC). During its development, the original flexible linker was modified into a more rigid structure, using piperidine and piperazine connections, which significantly increased its metabolic stability and therapeutic potency. The same linker design has also been used for the synthesis of the PROTAC drug, ARV-417, which is undergoing evaluation in a Phase 3 trial. Additional examples are shown in Table 1 and Table S1.

The photo-caged PROTAC linkers feature photosensitive groups that can be triggered to undergo irreversible photo-cracking reactions, after exposure to specific wavelengths of light⁴⁵. Using light, the linker’s protective group is effectively removed, resulting in the biodegradation of the targeted protein. This type of linker in PROTACs addresses the problem of off-target toxicity. The resulting PROTACs use a prodrug design strategy, enabling selective activation within target tissues. Xue et al.⁴⁵ introduced the bulky DMNB photocage structure to the linker of the potent PROTAC dBET1, creating the groundbreaking photocaged PROTAC (pc-PROTAC), that biodegraded the protein, bromodomain-containing protein 4 (BRD4). When exposed to light at 365 nm, pc-PROTAC efficiently generated dBET1 and produced the biodegradation of BRD4 in cells. This approach offers a promising strategy for achieving selective biodegradation of target proteins while minimizing the off-target adverse effects.

The photo-switchable PROTAC linkers use azo groups, rather than alkyl or polyether fragments, to attach the POI’s ligand to the moiety, which recruits E3 ligase⁴¹. Following exposure to specific wavelengths of light, these linkers cause the resulting PROTACs to suffer reversible photoisomerization within their *trans* and *cis* isomeric variants. This allows for precise and bidirectional control over PROTAC biodegradative efficacy⁴². The predicted influence of PROTAC conformational changes, induced by alteration in the linker conformation, on protein biodegradation determines the regulating effect. For example, Pfaff et al.⁴³ developed the first-in-class photoPROTACs that included a linker made of *ortho*-F4-azobenzene fragments introduced within the ligand of the BET protein, and the moiety recruited by the E3 ligase, van Hippel-Landau (VHL). These linkers allow for the continuous spatio-temporal control of the biodegradation of BET proteins by using wavelengths of 415 nm and 530 nm, minimizing the systemic toxicity produced by traditional anti-cancer drugs. Other examples are listed in Table 1.

Other infrequent rigid linkers in PROTACs include those based on aromatic, spiro, fused heterocycles, and macrocycles. The phenyl structure is present in the aromatic-based linkers, and thus far, only 10 related papers have been published⁸⁸. Four papers

have been published about spiro-based linkers containing structures, such as 7-azaspiro[3.5]nonane⁵⁸, or 3,9-diazaspiro[5.5]undecane⁵⁹. Three papers have been published regarding the fused heterocycle-based linkers, such as benzo[d]imidazole¹⁰² or cyclohepta[d]pyridazine⁴⁸. Furthermore, one paper described the synthesis and characterization of a macrocyclic-based linker, which was developed using a computer-aided drug design strategy⁶⁰. These rigid linkers are designed to increase the stability of PROTACs by stabilizing their structural and metabolic properties. Overall, these structures have good compatibility with other structural groups^{87,103,104}. By decreasing the reconfiguration of the bind conformation of the ligands to that of POI or E3 ligase, they can maintain the initial interaction¹⁰⁵. They form stacking interactions with the POI or E3 ligase, which increases the stability of the POI-PROTAC-E3 ternary complex and increases the biodegradation potency of the resulting PROTACs⁸⁸. For example, Li et al.¹⁰⁶ discovered a first-in-class phosphoinositide kinase PIKfyve biodegrader, PIK5-12d, which had an aromatic-based linker. PIK5-12d selectively induced PIKfyve biodegradation that was dependent on VHL and proteasome. The introduction of a phenyl ring in the linker maintained the aromaticity of the pyridyl group in the POI ligand, which may contribute to its binding with the PIKfyve protein, producing the highest PIKfyve biodegradation activity. Additional examples are shown in Table 1.

2.4. Linker characteristics

The examination of the structure–activity relationship (SAR) of PROTACs highlights the significance that specific linker characteristics involved in their function (Fig. 2C). The length of the linker significantly affects the establishment and stability of the POI-PROTAC-E3 complex^{4,51,68,142,143}. The type of group within the linker significantly affects pharmacokinetic properties^{6,29,64}. Furthermore, the linkage site of the linker significantly affects protein–protein interactions^{144–146}. In summary, linker characteristics have a significant impact on PROTAC biodegradation efficacy by modifying interactions between the PROTAC, POI, and E3 ligase.

3. Reasonable design and optimization strategies for PROTAC linkers

3.1. Basic strategies

Typically, PROTAC linker design and optimization rely on empirical or computer-aided methods. These methods play a fundamental role in drug development^{81,147–149}. Initially, researchers design PROTACs based on prior experience and then focus on optimizing the linker in four key areas: 1) adjusting the linker length to achieve an optimal configuration for a specific PROTAC¹⁵⁰, 2) modifying the type of linker group to balance the hydrophilic and hydrophobic properties in the PROTAC¹⁵¹, 3) modifying the flexibility of the linker and linkage site, to increase the stability of the ternary complex involving the POI, PROTAC, and E3 ligase^{120,152}, and 4) designing and synthesizing a diverse set of PROTACs with distinct linkers. This can also be accomplished using a computer-aided *de novo* approach¹⁹. The initial step involves determining the binding modes of the POI with its ligand and E3 with its ligand, respectively, using crystallography or molecular docking¹⁹. Subsequently, obtaining global protein–protein docking simulations using Molecular Operating

Environment (MOE), Rosetta, PatchDock, or other computational software, an ensemble of modeled structures of the POI-ligand and E3-ligand are generated. Following evaluation using molecular dynamics (MD), a reasonably modeled structure is used to analyze the protein–protein interactions (PPIs) and identify proteins interacting proximal to their ligated pockets. This is followed by the linker design process, where varying linkers are designed to generate a series of POI-PROTAC-E3 conformers. The ternary complex undergoes a restrained minimization protocol to eliminate steric hindrance between the PROTAC and proteins, allowing for the selection of an optimal linker for PROTAC synthesis. The rationality of the designed linker is ultimately verified through *in vitro* and *in vivo* experiments¹⁵³. Additional analysis of the structure–activity relationship (SAR) and the binding mode of the ternary complex, either through modeling or crystal structure, can guide the optimization of the linker, ultimately leading to the optimal linker (Fig. 3A)^{154–157}.

This strategy is widely applicable for linker design and optimization, particularly during initial efforts without knowledge of the binding mode of the ternary complex^{158,159}. However, this approach has certain limitations. One significant disadvantage is the synthesis of PROTACs^{160,161}. Nevertheless, this approach typically necessitates synthesizing multiple PROTACs with various linkers to comprehensively understand the SAR, which can be time-consuming, labor-intensive, and costly¹⁵⁵. Another limitation is the accuracy of theoretical predictions, particularly those related to protein–protein docking, which affects the design of the linker¹⁶². Sun et al.¹³⁰ made a significant discovery in the treatment of breast cancer. Using a SAR investigation aimed at examining various linker lengths and compositions, they created the first PROTAC biodegrading of the protein polo-like kinase 4 (PLK4) that is highly powerful, selective, and effective. This innovation was achieved by conjugating PLK4 ligand to a CCRN ligand thalidomide analogue, using various linkers. Initially, they designed and synthesized PLK4 PROTACs, connecting them with even-carbon chains ranging from 2 to 18 carbon-chain lengths, to determine the optimal range for the linker length. Their results indicated that the biodegradation of PLK4 was maximal when the carbon length of the PROTACs as 4 to 8 carbon atoms. Next, they examined the influence of a rigid linker on biodegradative efficacy, given that an inappropriate linker rigidity produces unfavorable angles that prevent binding with the CCRN protein. They discovered that the angle of the rigid linkers may be efficiently changed by introducing a carbonyl group between the linker and the PLK4 ligand, which increased the binding affinity of PLK4 and significantly increased the efficacy of PLK4 biodegradation. Finally, they developed the first *in vivo* efficacious PROTAC, SP27, using a linker that had a greater number of conformational constraints. This innovative PROTAC offers a promising candidate for characterizing PLK4-dependent biological functions and treating TRIM37-amplified breast cancer.

3.2. Cutting-edged strategies

In recent years, several cutting-edged design strategies for PROTAC linkers have emerged that primarily use artificial intelligence (AI) technology to improve the accuracy of PROTAC linker design^{163–169}. These methods are based on the utilization of existing knowledge. The general processes involve data collection, feature extraction, selection of suitable machine learning models, model training, validation, and application¹⁶⁶. Initially, a comprehensive dataset of known PROTAC linkers is collected,

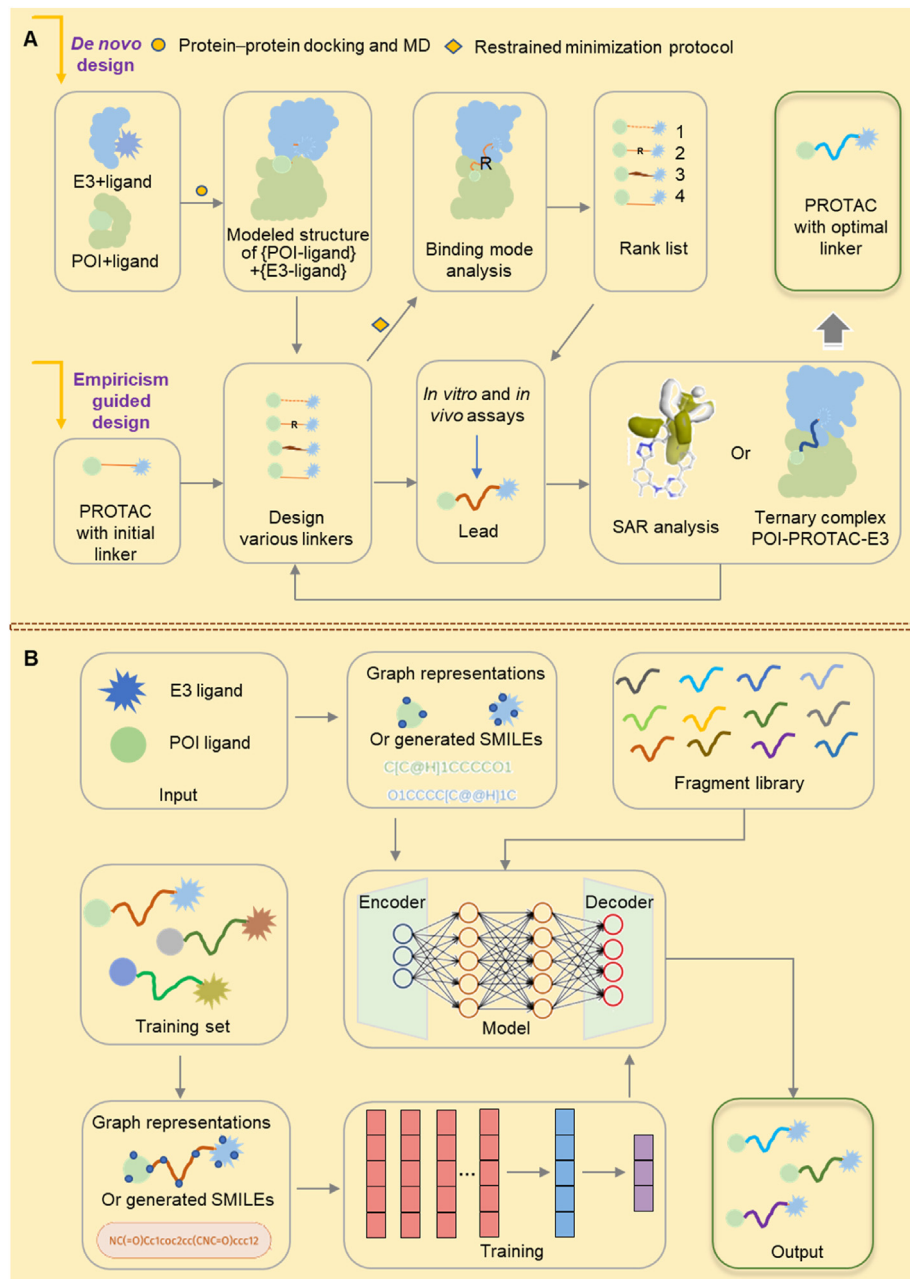


Figure 3 Appropriate design and optimization strategies for PROTAC linkers. (A) A standard protocol for the fundamental strategies of PROTAC linker design and optimization, which encompasses empirical design, *de novo* design using computational modeling, and further structural optimization through SAR analysis or the ternary complex binding mode of POI-PROTAC-E3. (B) Machine learning-based strategies for PROTAC linker design and optimization, which utilized existing knowledge of PROTAC linkers to train a model for rational PAROTC linker design.

encompassing their structures, efficacies, cellular penetration capabilities, and stability. This dataset is then utilized to train and validate the machine-learning models. Next, the pertinent chemical and physical properties are extracted from the structure of the PROTAC linker which may encompass the types of atoms and bonds, molecular weight, and electrical distribution, among others. Subsequently, suitable machine learning models, such as deep neural network (DNN)¹⁷⁰, transformer neural network¹⁶⁶, or recurrent neural network (RNN)¹⁶³ are chosen and trained using the extracted features and known experimental data. By carefully

adjusting the model's parameters and optimizing the underlying algorithm, the prediction accuracy and generalization are increased. An independent test dataset is used to evaluate the predictive performance of the trained model. Finally, the trained model is utilized to predict a novel PROTAC linker (Fig. 3B).

The integration of machine learning algorithms into PROTAC linker design enables rapid extraction of patterns from vast datasets, expediting the design process, increasing success rates, minimizing experimental iterations, and mitigating financial expenses¹⁷¹. Nonetheless, this approach possesses certain

limitations, such as the caliber and volume of data impact the efficacy and precision of the model. As an instance, Kao et al.¹⁷⁰ used cutting-edge techniques to introduce AIMLinker, a deep neural network that facilitates the rapid design and creation of novel PROTAC linkers. AIMLinker accepts two unconnected fragments as inputs and uses an encoder-decoder deep learning architecture to generate the substructures that constitute a novel PROTAC molecule. Subsequently, it conducts postprocessing on compounds that are produced to find possible candidates for drugs. It checks for repeats and ignores structures that contain unwanted substructures or defy basic chemical rules. This streamlined process allows for the timely generation of new small molecules that have strong affinity for binding CRBN-BRD4 and its adaptability for application to other PROTAC targets. Additional machine learning strategies are summarized in Table 2.

4. Effects of linker characteristics on the biodegradation efficiency of PROTACs

4.1. Linker length affects the formation of ternary complex

The linker length has a pivotal effect on determining the biodegradation efficacy of PROTACs. It affects the formation of the ternary complex, as illustrated in Fig. 4A^{68,142,143}. The optimal linker length depends on the interaction pattern, distance, and spatial structure of the ternary complex¹⁵¹. Prior studies have shown that an inappropriate linker can significantly decrease PROTAC bioactivity^{58,174}. If the linker is too long, it may weaken the interaction between POI and E3 ligase, decreasing the probability of a stable ternary complex formation. Conversely, a shorter linker may introduce steric hindrance, disrupting ternary complex formation, and decreasing the biodegradation efficacy of PROTAC^{58,174}. Therefore, achieving an optimal linker length is essential to produce maximal interactions between the POI and E3 ligase, leading to effective ubiquitination and biodegradation of the POI.

To demonstrate how linker length affects PROTAC efficiency, a study used the PROTAC ZZ151, which promotes the biodegradation of the protein, Son of Sevenless Homologue 1 (SOS1)¹¹¹. SOS1 plays a crucial role in the activation of the oncogene, Kirsten ras (KRAS), making it a promising target for KRAS-induced cancer treatment^{175,176}. Researchers have intended to develop effective inhibitors or complexes that biodegrade proteins for KRAS-driven cancers by regulating SOS1¹⁷⁷. One study focused on determining the relationship between linker length and PROTAC efficacy, leading to the discovery of the PROTAC ZZ151¹¹¹. Initially, inhibitor-based SOS1 PROTACs were developed that sequestered the E3 ligase VHL (von Hippel-Lindau)¹⁷⁸. The initial SOS1 inhibitor, analog 7¹⁷⁹, with an *N*-acetyl piperidine group, was an appropriate attachment site for the VHL ligand. Alkyl-based linkers were used to connect the SOS1 ligand, 7, to the VHL ligand, generating a series of PROTACs (8a–g) containing 3 to 9 methylene units (Fig. 4B). The effect of PROTAC efficacy was determined by varying the linker length. The efficacy of PROTACs 8 in inducing the biodegradation of SOS1 in non-small cell lung cancer cells (NCI-H358) was evaluated. The results indicated a significant correlation between the length of the linker and the efficacy of the PROTACs 8a–g, containing 3 to 9 methylene units. Among these, PROTAC 8c (ZZ151), with a linker that contained five methylene units, had the most potent activity, producing

complete SOS1 biodegradation, at a half-maximal degradation concentration (DC_{50}) of 15.7 $\mu\text{mol/L}$ and a maximal biodegradation efficacy (D_{\max}) of 100% (Fig. 4C). In mice xenografted KRAS^{G12D}-mutant cancer cells, the PROTAC ZZ151 produced a dose-dependent decrease in SOS1 biodegradation (Fig. 4D), producing corresponding decrease in the levels of phosphorylated ERK (pERK) (Fig. 4E). In contrast, PROTACs 8b and 8d, containing four and six methylene units, respectively, were less potent than 8c. The relationship between the biodegradative efficacy of PROTACs for SOS1 and the ternary complex POI-PROTAC-E3 formation was determined using a homogeneous time-resolved fluorescence (HTRF) assay. PROTAC ZZ151 produced the highest HTRF signal and ternary complex formation. Other compounds with lower biodegradation efficacies produced weaker HTRF signals, indicating a lower propensity for ternary complex formation (Fig. 4F). In summary, the highly potent PROTAC ZZ151 was developed using meticulous linker length optimization. This compound effectively and rapidly produced the biodegradation of SOS1, indicating that it might represent a therapeutic approach to treating KRAS-driven cancers.

An analysis of the above examples highlights the significant effect of linker length on the biodegradation activity of PROTACs. Indeed, small variations in length produced significant alterations in efficacy. For example, this study identified an optimal 5-carbon chain length, as shorter or longer chains produced a lower magnitude of biodegradation efficacy. When the carbon chain was increased by 7 methylene units, the biodegradation efficacy was increased, and the corresponding HTRF signal was slightly weaker than that for an 8-carbon chain. This may be due to differences in spatial conformations of the linker, which can be determined by examining the crystal structure of the ternary complex. Therefore, in the design of PROTACs, careful consideration of linker length is paramount. A reasonable range of linker lengths should be established, typically spanning 5 to 15 carbon chain lengths. A detailed evaluation is essential and varying the number of carbon atoms one at a time is required to accurately identify optimal lengths. The length of a linker is intricately linked to ternary complex formation and, ultimately, biodegradation efficacy. Consequently, optimizing linker length is essential for the efficient identification of highly efficacious PROTACs.

4.2. The group type of the linker affects the cell permeability of the PROTACs

The group type of linker between the binding and recruiting moieties in PROTACs significantly affects their biodegradative efficacy^{105,180–182}. This is due to the linker's chemical composition, which directly affects the physicochemical properties of the PROTAC, including its molecular weight (MW), hydrogen bond donors (HBDs) and acceptors (HBAs), octanol–water partition coefficients ($clogP$), hydrocarbon–water partition coefficient ($\log D_{\text{dec/w}}$), and solubility^{149,180}. These factors, in turn, significantly affect the PROTAC's cell permeability (Fig. 5A)¹⁸³. For example, as the MW increases, cell permeability generally decreases¹⁸⁴. When the MW exceeds 1000 Da, there is a significant decrease in cellular permeability^{185,186}. Furthermore, PROTACs with fewer HBDs and HBAs have a higher magnitude of cell permeability. However, introducing a solvent-exposed HBD can decrease cell permeability¹⁸⁷. The lipophilic permeability efficiency (LPE) measures how well a PROTAC permeates a cell

Table 2 Innovative models for the design and development of PROTAC linkers.

Model	Method	Principle	Characteristic	Ref.
PROTAC-INVENT	Reinforcement learning (RL)	The model is jointly trained using the RL approach, aiming to direct PROTAC structure generation towards predefined 2D and 3D properties.	It can not only generate PROTAC SMILES, but it can also calculate their possible three-dimensional bind conformations in conjunction with POI and E3 protein.	163
DeLinker	Graph-based deep generative model (Gated Graph Neural Network (GGNN))	The model combines structural knowledge with machine learning approaches, utilizes two fragments or partial structures, and generates a molecule that incorporates both.	This is the inaugural molecular generative model that incorporates 3D structural information directly into the design process, successfully demonstrating its efficacy and applicability in PROTAC design.	165
FFLOM	Deep generative model (graph convolutional network (GCN))	The model typically adjusts the fragment and generation lengths, optimizing the local fragment while preserving the dominant region and its conformation.	During the PROTAC design process, the model not only replicates the experimentally verified baseline molecule but also generates numerous novel structures with superior binding affinity scores.	167
AIMLinker	Deep learning (deep neural network (DNN))	The model retrieves structural data from input fragments and creates linkers for their integration.	It can rapidly design and generate linkers to create drug-like PROTACs with improved chemical properties.	170
Link-INVENT	Reinforcement learning (RNN)	The model takes two molecular subunits with a defined exit vector and a pair of warheads. It then produces a linker and outputs the connected molecule in SMILES format.	The model generates optimal linkers that connect molecular subunits and fulfill various goals, making it easier to use the model in practice for PROTAC design.	168
3DLinker	Conditional VAE-based generative model (vector neuron networks)	The model has the ability to predict anchor atoms and generates invariant graphs and equivariant absolute coordinates of linkers given two 3D fragments.	The model has a significantly higher rate of recovering molecular graphs and accurately predicting the 3D coordinates of all atoms.	164
ShapeLinker	Reinforcement learning (RNN)	The model implements fragment linking using reinforcement learning on an autoregressive SMILES generator.	The model generates linkers that satisfy relevant 2D and 3D criteria, achieving top-notch results in generating novel linkers under a predefined linker conformation.	169
DRlinker	Deep reinforcement learning (transformer neural network)	The model manages the linking of fragments by exploring the desired chemical space for novel molecules with anticipated properties.	The model is effective for various tasks, ranging from controlling linker length and $\log P$ to optimizing the predicted bioactivity of compounds and addressing various multiobjective challenges.	166
PROTAC-RL	Reinforcement learning (RL) (transformer neural network)	The model, utilizing generative deep learning, incorporates a robust transformer architecture along with memory-enhanced RL to create highly effective PROTACs. It accepts E3 ligands and warheads as input and generates linker sequences that produce chemically feasible PROTACs with superior properties.	It not only enables the rational design of PROTACs in limited resource settings but also guides the selection of PROTACs with the most favorable pharmacokinetics.	172

Table 2 (continued)

Model	Method	Principle	Characteristic	Ref.
DeepPROTAC	Deep neural network model (graph convolutional network)	In the model, ligand and ligand binding pockets are represented using graphs and fed into GCNs for feature extraction. Linkers are represented using SMILES notation to generate features for rational PROTAC design.	It not only can achieve rational PROTAC design but also can estimate the biodegradation activity of the resulting PROTAC based on the targeted POI and E3.	173

membrane through passive diffusion, at a specific lipophilicity level. A decrease in LPE results in lower cell permeability¹⁸⁸. Therefore, selecting the appropriate group type of linker is crucial for optimizing the PROTAC's physicochemical features, which can significantly impact its cell membrane permeability.

To illustrate the effect of the linker group type on cell permeability, we compared two PROTACs, MZ1 and MZ3^{27,68}, which target the bromodomain and extra-terminal domain (BET) protein. BET regulates the expression of certain genes and it has been suggested that it may be a therapeutic target for various diseases^{189–192}. The PROTACs were developed based on a comprehensive study examining the effect of the linker group type on PROTAC efficacy^{27,68}. The MZ series, composed of the BRD4 inhibitor, JQ1¹⁹³, and the VHL binder, VHL-1¹⁹⁴, used distinct linkers to join the two compounds. The connection points of the linkers were determined by analyzing the crystal structures of BRD4 complexed with JQ1 and VHL with VHL-1. The solvent-exposed *t*-butyl ester of JQ1 and the acetyl methyl of VHL-1 were suitable for linker attachment. MZ1 contained a PEG-based linker with three ethylene glycol units, whereas MZ3 used the same linker with an additional phenylalanine group between the ethylene glycol units and VHL-1 (Fig. 5B). The intracellular assay results indicated that MZ1, at 1 μmol/L, was the most efficacious compound, removing over 90% of BET proteins in HeLa cells. MZ3 produced concentration-dependent biodegradation of BET proteins, achieving efficacy in HeLa cells at concentrations from 0.1 to 10 μmol/L (Fig. 5C). Permeability experiments indicated that MZ1 had significantly higher permeability ($P_e = 6 \times 10^{-7}$ cm/s), compared to MZ3 ($P_e = 6 \times 10^{-9}$ cm/s), primarily due to their distinct physicochemical properties. MZ1 had optimal physicochemical properties, including an MW of 959 Da, *clogP* of 3.7, HBDs of 4, HBAs of 11, $\log D_{\text{dec/w}}$ of -1.1, and LPE of 0.5. These properties contributed to its greater cell permeability and biodegradative efficacy. In contrast, introducing an additional phenylalanine moiety into the linker of MZ1, which produced MZ3 resulted in a MW exceeding 1000 Da and an increase in the solvent-exposed HBD count, which decreased cell permeability. Furthermore, modifications to the *clogP* and $\log D_{\text{dec/w}}$ values caused a significant decrease in the LPE value, further compromising cellular permeability (Fig. 5D). Collectively, these findings emphasize the critical role of linker group types in determining the physicochemical properties of PROTACs and their subsequent effect on cell permeability and biodegradative efficacy.

Obtaining a high magnitude of cell permeability and oral bioavailability for PROTACs represents a significant challenge, as these values are beyond the constraints defined by Lipinski's rule of five¹⁹⁵, approaching or even exceeding the outer limits of the oral beyond the rule of five (bRo5)¹⁹⁶. Previous studies have shown that PROTACs, utilizing CRBN and VHL ligands, had

median molecular weights of roughly 900 and 1000 Da, respectively, and have rotatable bond (ROB) counts of 20–30. The physicochemical characteristics of these PROTACs are similar to those for orally absorbed medications, as indicated by *clogP* values of 4–6 and HBD counts of 3–4. Notably, lipophilicities and HBD counts produce a greater effect on permeability compared to MW^{197,198}. Differences in HBD counts and *clogP* values within a series of PROTACs produce significant disparities in cell permeability. Therefore, a comprehensive evaluation of PROTAC permeability across a broader *clogP* spectrum can provide a lipophilicity profile that can guide the development of PROTACs that have increased cell permeability.

4.3. Linker flexibility affects the stability of the ternary complex

The flexibility of the linker is a critical factor in determining the biodegradative efficacy of PROTACs by modifying the stability of the ternary complex (Fig. 6A)^{6,29,64}. It is essential to consider linker flexibility during PROTAC design⁸⁵. A linker with significant conformational flexibility can enhance interactions between the PROTAC, POI, and E3 proteins, preventing stable binding at a fixed interface⁸⁵. Conversely, introducing rigid groups into a flexible linker can enhance stiffness and replicate the original geometry of the PROTAC, leading to new interactions and increased stability of the ternary complex²⁹. Therefore, it is beneficial to choose linkers with a certain degree of rigidity for use in PROTACs as they aid in stabilizing the POI-PROTAC-E3 complex, ultimately enhancing biodegradative efficacy.

In the following section, we will discuss the optimization process that was used for the PROTAC, Bavdegalutamide (ARV-110), and the impact of linker rigidity on the magnitude of the biodegradation of AR. Prostate cancer, which ranks second in frequency among cancers in males, is characterized by its dependence on abnormal AR signaling¹⁹⁹. Chronic exposure to androgen deprivation therapy (ADT) often produces castration-resistant prostate cancer (CRPC), where the AR is still a crucial oncogenic driver²⁰⁰. Clinical research has reported the therapeutic advantages of AR degraders for patients with colorectal cancer. ARV-110, developed by Arvinas, was the first PROTAC to get into clinical trials with an emphasis on AR, specifically for the treatment of metastatic CRPC⁹⁸. This PROTAC represents a prime example of the optimization process and the significance of linker rigidity in increasing AR biodegradation efficacy.

In the early design phase, the researchers evaluated various E3 recruiting ligands and AR binders. They ultimately selected PROTAC **1** as the lead compound for further structural optimization. PROTAC **1** consists of an AR ligand and the CRBN ligand, thalidomide, connected via an alkyl chain containing a piperazine ring. The initial step in optimization involved modifying the AR ligand of PROTAC **1**. The trifluoromethyl group was

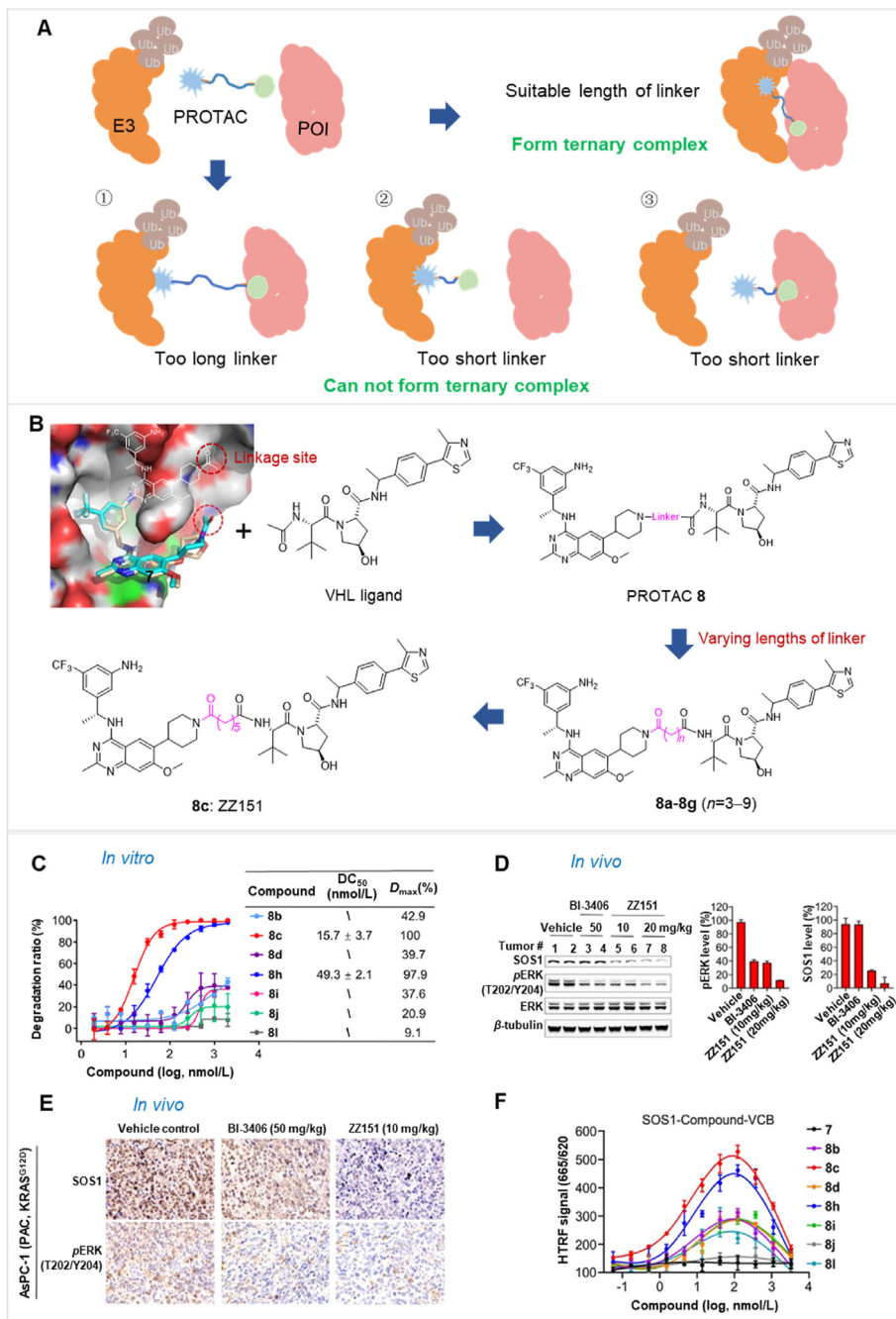


Figure 4 The impact of linker length on ternary complex formation. (A) The impact of linker length on the formation of the ternary complex between POI, PROTAC, and E3 is significant. An optimal linker length is essential for facilitating this ternary complex formation. (B) The design strategy for PROTAC 8 primarily focuses on optimizing linker length. (C) PROTAC 8C (ZZ151) exhibits the most potency in terms of biodegradation activity for SOS1. (D) After 21 days of treatment, the expression levels of SOS1 and pERK were quantified in AsPC-1 xenograft pancreatic cancer cells in mice. PROTAC 8C (ZZ151) at 10 and 20 mg/kg, BI-3406 (SOS1 inhibitor) at 50 mg/kg, and vehicle (DMSO) were administered. PROTAC 8C (ZZ151) was most effective in reducing the expression levels of SOS1 and pERK. (E) An immunohistochemistry assay was conducted to assess SOS1 and pERK levels in AsPC-1 xenograft tumors. (F) Minor modifications to the linker can significantly influence the formation of the ternary complex between SOS1, PROTAC, and VCB, as determined by HTRF assay results. The lead biodegradable compound, PROTAC 8C (ZZ151), exhibited the greatest maximal ternary complex formation. Reprinted with permission from Ref. 111. Copyright©2023 American Chemical Society (Supporting Information Fig. S1).

replaced with chlorine atoms and a pyridinyl ring replaced the phenyl ring to increase the likelihood of hydrogen bond formation. The piperazine groups in the linker were directly connected to the AR ligand, while maintaining the length of the linker,

yielding PROTAC 2. This compound could represent a potential candidate for further optimization. The next phase of optimization involved modifying the AR ligand. The pyridinyl group was replaced with a pyrimidine ring, introducing a piperidyl group

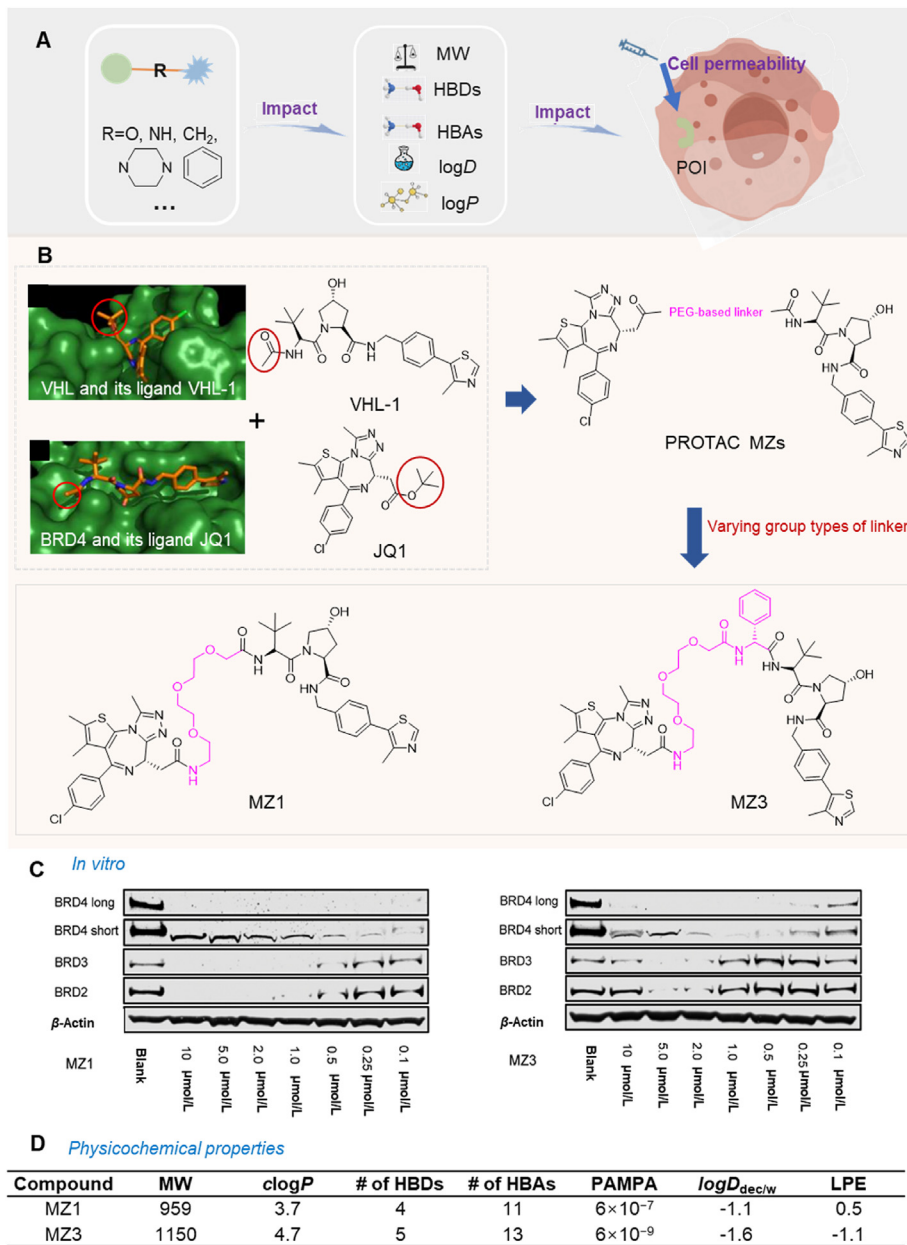


Figure 5 The linker group type's impact on PROTAC cell permeability. (A) The linker group type significantly impacts the cell permeability of PROTAC. This effect is primarily due to its influence on the physicochemical properties of PROTAC, ultimately determining its cell permeability. (B) The design strategy for PROTAC MZs primarily focuses on the insertion of different groups into the linker to alter the physicochemical properties of PROTAC. (C) HeLa cells incubated with different concentrations of MZ1 (left) and MZ3 (right) demonstrate selective biodegradation of BRD4. MZ1 is the most efficacious compound, removing over 90% of all BET proteins even at a concentration of 1 $\mu\text{mol/L}$. Reprinted with permission from Ref. 27. Copyright ©2015 American Chemical Society (Supporting Information Fig. S2). (D) The physicochemical properties of PROTAC MZs indicate that inserting different groups into the linker of PROTAC can significantly influence its physicochemical properties, leading to notable differences in cell permeability. MZ1, with an MW < 1000 Da, fewer solvent-exposed HBD and HBA, suitable $c\log P$ and $\log D_{\text{dec/w}}$, and LPE value, demonstrate higher cell permeability.

that decreased the flexibility of the linker and this increased its hydrogen bonding capacity, yielding PROTAC 3, which had significant biodegradation efficacy *in vitro*. The addition of piperidyl to the linker limited the rigidity of the PROTAC, thus allowing for the original binding mode of the AR ligand, AR, thalidomide, and E3, thereby producing biodegradation efficacy. Subsequently, PROTAC 4 was developed by replacing the pyrimidine ring in the AR ligand with a phenyl ring, which decreased the number of

hydrogen bond donors. Finally, the substituted cyclobutane in the AR ligand was replaced with cyclohexane and this modification increased the PROTAC's rigidity but decreased its TPSA. Finally, the replacement of the phenyl group with pyridazine increased the hydrogen bonding interactions and retained the unchanged linker, yielding ARV-110 (Fig. 6B)²⁰¹. The oral administration of ARV-110 was efficacious in producing the biodegradation of the wild type and the antiandrogen therapy-induced mutant forms of AR.

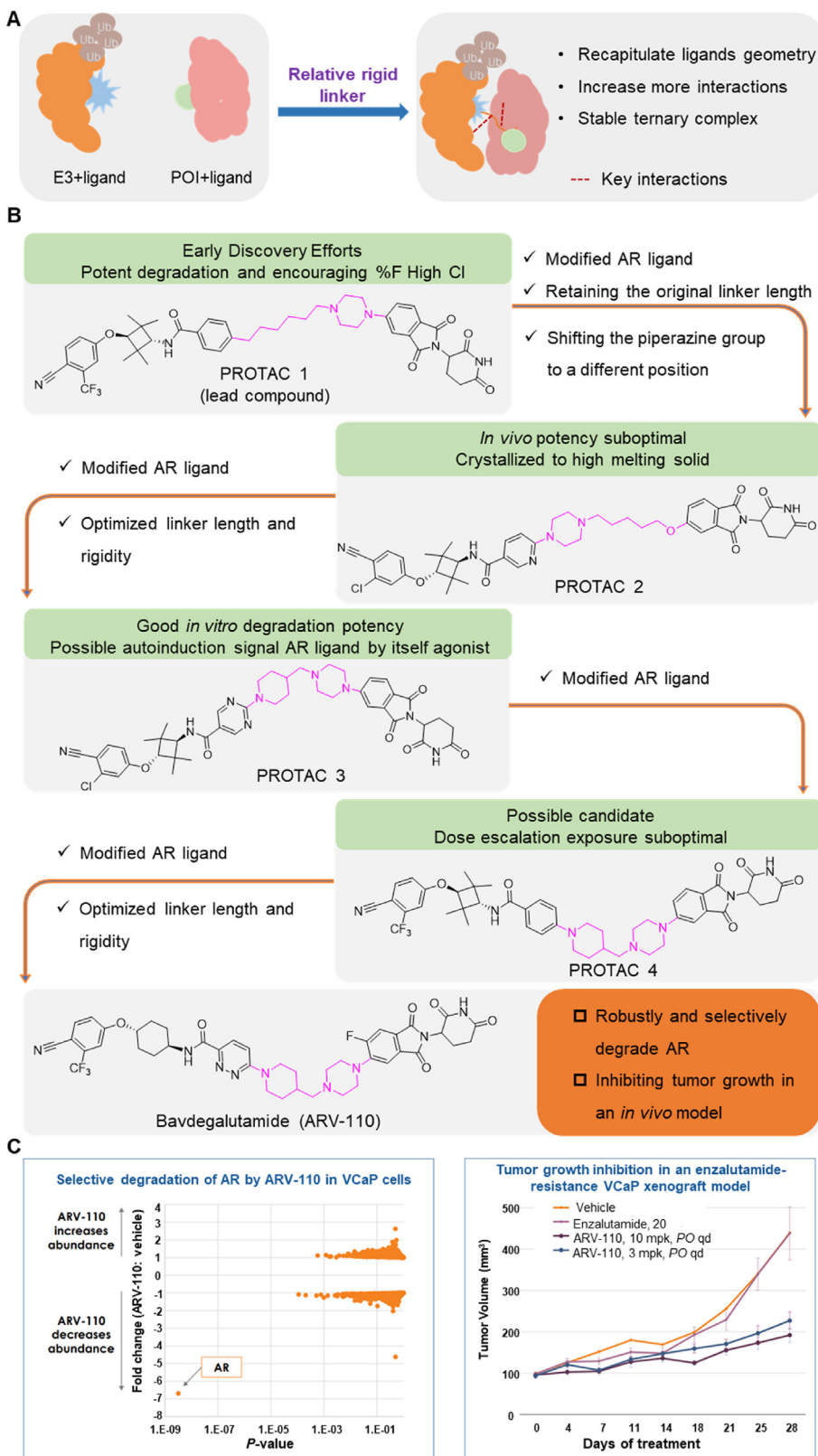


Figure 6 The effect of linker flexibility on PROTAC stability. (A) Linker flexibility has an impact on PROTAC stability. A more stable ternary complex enhances PROTAC efficacy. (B) The design approach for the discovery of PROTAC ARV-110 emphasizes linker flexibility and AR ligand optimization. (C) ARV-110 selectivity was evaluated by proteomics. After treating VCaP cells with 10 nmol/L ARV-110 for 8 h, AR was the only protein among nearly 4000 proteins. (D) Daily oral administration of ARV-110 significantly inhibited tumor growth. A 10 mpk dose resulted in 70% tumor growth inhibition.

ARV-110 is capable of biodegrading 95%–98% of AR among various prostate cancer cells. ARV-110 also decreases tumor growth by 70%–100% in drug-resistant mouse models (Fig. 6C)²⁰². Preliminary data from Phase I clinical trials indicated that ARV-110 has satisfactory safety and tolerability profiles.

The researchers developing ARV-110 initially focused on the linker segment. They evaluated various linker lengths, increased linker rigidity, and modified the AR ligand to obtain ARV-110. The examination of the crystal structure of CCRN and thalidomide indicated that the isoindoline of thalidomide, towards the solvent-exposed region, created a stacking interaction with the neighboring amino acids of CCRN²⁰³. This observation suggested that a rigid linker connected to this isoindoline would increase thalidomide's binding interaction with CCRN, by maintaining its original binding mode. Furthermore, the aromatic ring of the AR ligand, which was exposed to the solvent region, formed a stacking interaction with Thr877 in the AR protein²⁰⁴. The rigid linker component, directly connected to this aromatic ring, appeared to increase the stability of the AR ligand's binding mode within AR. Based on the interaction modes of the AR ligand with AR and thalidomide with CCRN, one could conclude that the rigid linker is essential for maintaining their binding modes, increasing the stability of the ternary complex, producing the biodegradation efficacy of ARV-110. During the design of the linker, it is crucial that the linker maintains a rigid structure when POI and E3 ligands accumulate in the solvent-exposed region and form engaging in stacking interactions. By maintaining a rigid linker, it may be easier to ensure the stability of the ternary complex, ultimately yielding the biodegradation efficacy of PROTACs.

4.4. The linkage site of the linker affects the protein–protein interactions

The linkage site of the linker plays a significant role in determining the biodegradative efficacy of PROTACs by affecting the interaction of POI and E3 (Fig. 7A)^{144–146}. The optimization of PROTAC linkers often involves identifying the most favorable site for structural derivatization, thereby ensuring that the maximal binding affinity is retained²⁰⁵. This selection process typically involves analyzing the solvent-exposed regions of the protein–ligand interaction interfaces^{145,146}. When a PROTAC linker cannot be extended, it limits the POI ubiquitination efficacy of the E3 ligase²⁰⁶. By introducing an optimal linker linkage in a solvent exposure region, protein–protein interactions can be maximized, while preserving the original ligand interactions with the POI or E3 ligase²⁰⁵. Furthermore, an appropriate linker can establish alternative interactions with the POI, increasing ternary complex stability¹. Overall, selecting the linkage site in the PROTAC linker is a crucial decision that can directly impact PROTAC's biodegradative efficacy and selectivity.

We will discuss the discovery of PROTACs, SJF α , and SJF δ ¹⁴⁷, which can produce the biodegradation of the p38 Mitogen-activated protein kinase (MAPK). This discussion will illustrate the significance of the linkage site of the linker on the efficacy of PROTACs. The p38 MAPK pathway is a crucial regulator of pro-inflammatory cytokines biosynthesis at the transcriptional and translational levels. Thus, modulation of this pathway by pharmacological compounds could represent treatment for autoimmune and inflammatory diseases^{207,208}. The p38 MAPK kinases, consisting of α , β , γ , and δ isoforms, are activated by environmental stress and cytokines. These kinases exhibit distinct

expression patterns in different tissues^{208,209}. The PROTACs, SJF α and SJF δ , were discovered based on foretinib²², a kinase inhibitor, and the VHL protein serving as an E3 ligase. The linkage site connecting the VHL ligand and foretinib was meticulously optimized to increase their biodegradative efficacy for the related kinase isoforms¹⁴⁷. The authors, through the crystal structure of VHL and its ligand, identified two distinct groups in the solvent-exposure region that could serve as linkage sites^{67,210}. They synthesized the “amide series” of PROTACs, using the known amide of VHL ligand as the linkage point for the linker to foretinib⁶⁷. In contrast, the “phenyl series” of PROTACs used an under-explored phenyl group as the attachment site²¹⁰. Both series utilized the same phenyl ether of foretinib as the linkage site, connecting it with different lengths of linkers (Fig. 7B). In the “amide series”, the PROTAC with a 13-atom linker (SJF α) was highly selective in biodegrading p38 α ($D_{max} = 97.4\%$, $DC_{50} = 7.16$ nmol/L). However, it was significantly less efficacious in biodegrading p38 δ ($D_{max} = 18\%$, $DC_{50} = 299$ nmol/L). In contrast, in the “phenyl series”, decreasing the linker length to 10 atoms yielded the PROTAC SJF δ , which selectively biodegraded p38 δ ($D_{max} = 99.41\%$, $DC_{50} = 46.17$ nmol/L), without biodegradation p38 α , β , or γ . The foretinib-based PROTAC had a weak binary affinity for p38 α . Nonetheless, the obstacle was surmounted through the collaborative interactions within VHL and p38 α , ultimately leading to a heightened affinity of SJF α for p38 α with VHL²². Similarly, the affinity of SJF δ for p38 δ and VHL is 436 nmol/L, representing a tenfold increase, compared to the affinity of the VHL-PROTAC complex. The ternary complex has a higher binding capacity than the binary complex due to the extra PPIs within VHL, p38 α or p38 δ , and SJF α or SJF δ , respectively. Furthermore, the affinity of the p38 δ -SJF α -VHL and p38 δ -SJF δ -VHL complexes was also determined, and the results indicated that the SJF δ complex is approximately 3-fold stronger than the SJF α complex (Fig. 7C). To determine the structural basis for the variation in ternary affinity among the p38 δ -SJF α -VHL and p38 δ -SJF δ -VHL complexes, molecular dynamics simulations were conducted. The results indicated that with SJF α , the interaction between Arg108 of VHL and Lys220, Thr221 of p38 δ was unfavorable. In contrast, with SJF δ , Arg108 of VHL and Glu49, Glu160 of p38 δ produced a favorable stabilization of the ternary complex (Fig. 7D). These findings suggest that the linkage site and linker length influenced the formation of distinct ternary interfaces, leading to inherent differences in ternary complex affinity. These differences ultimately enable selective biodegradation by different PROTACs.

The objective of the p38 PROTACs study was to create isoform inhibitors of p38 MAPKs by utilizing a single E3 ligand and a single POI ligand. By manipulating the linker design of PROTACs and producing a distinct orientation of the recruited E3 ligand while maintaining a consistent warhead, this approach allows for the selective biodegradation of a specific isoform of a protein family¹⁴⁷. This study highlights the significance of linker linkage site selection in PROTAC design. Typically, linker design involves selecting solvent-exposed regions based on crystal structures. However, it is also essential to consider the ease of synthesizing linkers at these sites. For complexes without crystal structures, molecular docking is often employed to determine the binding mechanism of POI with its ligand, as well as E3 and its ligand, thereby aiding in the selection of linker linkage sites. In conclusion, the selection of linker sites is crucial in PROTAC design, as it affects the ternary complex stability by influencing the interactions among POI and E3, ultimately influencing the degradation activity of PROTACs.

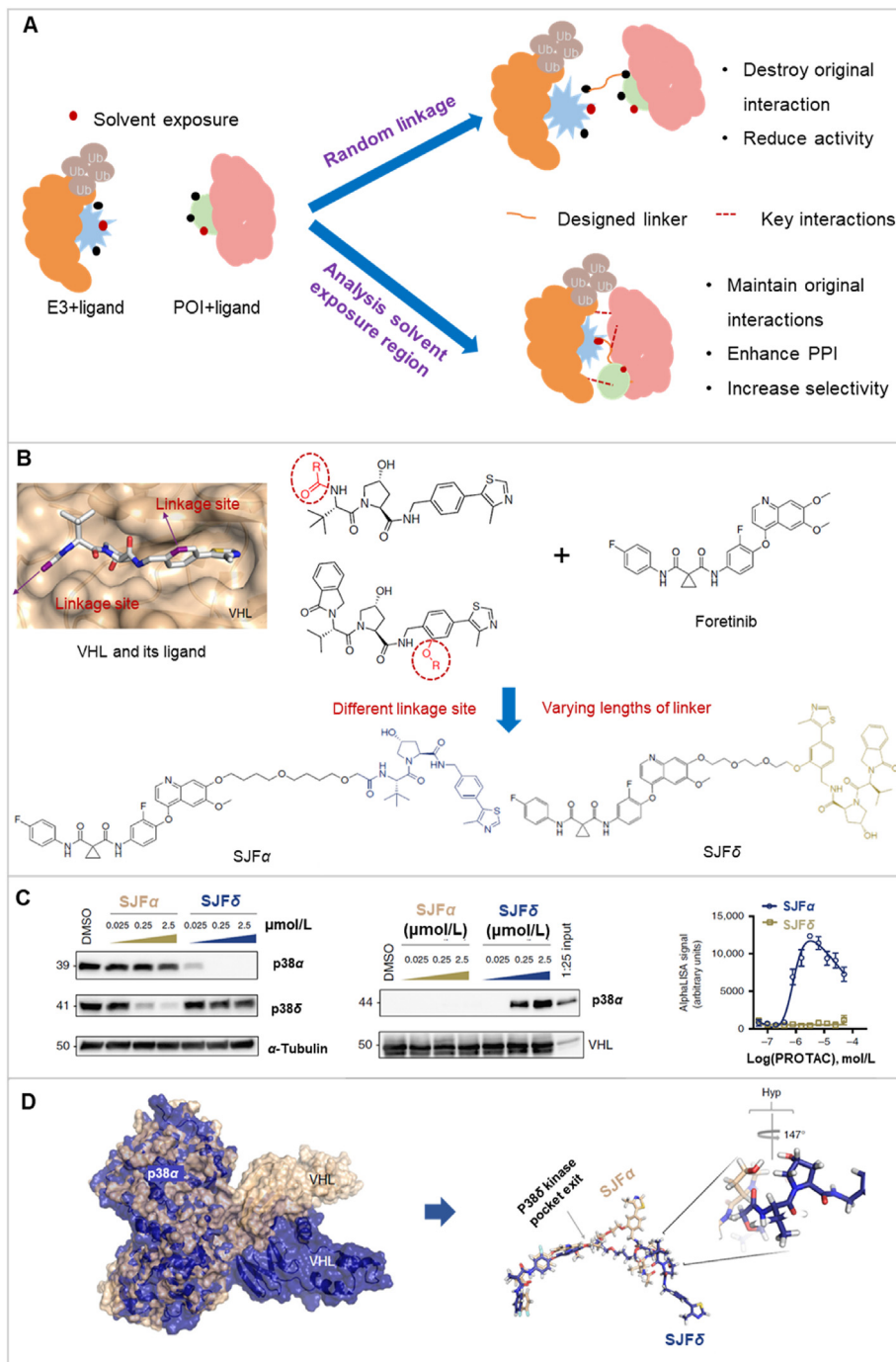


Figure 7 The effect of linkage site on protein–protein interaction (PPI). (A) The linkage site of the linker is essential for protein–protein interaction (PPI). An increase in PPI formation enhances the biodegradation efficiency. (B) The design approach for PROTAC SJF α and SJF δ emphasizes the optimization of the linkage site. (C) PROTAC SJF α preferentially biodegrades p38 α , while SJF δ preferentially biodegrades p38 δ . (D) Immunoprecipitation of GST-tagged VBC is only feasible when p38 α is incubated with PROTAC SJF α (left). The AlphaLISA assay indicates that p38 α , SJF α , and VHL form a substantial ternary complex; p38 α , SJF δ , and VHL do not create a ternary complex (right). Reprinted with permission from Ref. 147. Copyright ©2019 Nature Communication (Supporting Information Fig. S3). (E) Molecular dynamics simulations show distinct PPI contacts between p38 δ and VHL depending on whether they are recruited by SJF δ or SJF α .

5. Conclusions

In this review, we have summarized the types of PROTAC linkers, the design and optimization strategies used, and the impact of linker characteristics on PROTAC efficacy. As

previously mentioned, PROTAC linkers can be broadly classified into two groups: flexible linkers and relatively rigid linkers. Flexible linkers, which are prevalent in PROTAC design, often use a long and flexible structure^{29–31}. However, this design can increase the susceptibility to oxidative metabolism *in vivo*²¹¹. In

contrast, relatively rigid linkers have been less frequently used due to limitations in synthesis technology within the PROTAC field³⁷. Nonetheless, cycloalkane-based linkers, especially the inclusion of piperazine and piperidine components, are used as they increase the solubility and stability of the ternary complex. Triazole-based linkers are another frequently used rigid linkers, due to the advent of the “click” chemical reaction, using the copper-catalyzed 1,3-dipolar cycloaddition reaction, which offers high compatibility with different functional groups and a consistent reaction rate^{24,35,36}. Another type of linker, photo-controlled PROTAC linkers, such as photo-switchable PROTAC linkers, use azo fragments rather than alkyl or polyether fragments, causing the resulting PROTACs to undergo reversible photoisomerization when exposed to specific wavelengths of light⁴¹. This makes it possible to precisely and reciprocally regulate the rate of PROTAC biodegradation. Furthermore, researchers have developed different linker optimization strategies. The application of AI in PROTAC linker design has significantly improved the accuracy and efficiency of linker optimization¹⁷¹. By leveraging machine learning frameworks, researchers have gained insights into the structural, physical, and chemical properties of PORTAC linkers. These insights have been translated into practical applications, leading to more accurate PROTAC linker designs. Advanced AI techniques, such as deep learning and reinforcement learning, are expected to further enhance PROTAC linker design in the future^{63,162,212,213}. Furthermore, the linker’s four key characteristics: length, group type, flexibility and linkage site, were examined based on case studies. These characteristics are essential for influencing the stability of the ternary complex POI-PROTAC-E3, the cell permeability of PROTACs, the creation of the ternary complex, and the interaction between POI and E3. Consequently, they significantly affect the biodegradation efficacy of PROTACs²¹⁴.

Currently, there is a lack of precise quantitative descriptions for these characteristics. Based on available data from reported and clinically tested PROTACs, the typical length of atoms within the linker chain ranges between 5 and 15 atoms. Although a longer chain length can diminish activity due to increased entropy, this effect is generally less significant than the effect of a shorter molecular distance between ligand ends caused by a shorter chain length. Consequently, in the initial stages of PROTAC design, a slightly longer linker chain is often chosen. To increase the formation of ternary complexes, a flexible linker is chosen, allowing the PROTAC to adopt a suitable angle that facilitates the stable assembly of ternary complexes²³. Various chemical groups, including amino, carboxyl, and hydroxyl groups, can be introduced in the linker to increase the chemical diversity of PROTAC and its ability to traverse cell membranes²⁷. To facilitate subsequent chemical modification and optimization, it is essential for the linker to possess reactive functional groups or other modifiable sites. When selecting a linkage site, it is essential to consider the binding mode between the POI and ligand or E3 and ligand. The solvent-exposed region should be chosen, as it provides easy access for connecting groups²¹⁴. Overall, with appropriate linker optimization, a wide range of linkers can be designed to produce greater PROTAC potency. Additional linker characteristics will be discussed in future studies. Nevertheless, our primary focus remains on rationally optimizing the linker characteristics to enhance the biodegradative efficacy of the PROTACs.

Although optimizing the length, group type, flexibility and the linkage site of the linker can increase the efficacy of

PROTACs, several challenges must be overcome. Firstly, the structural complexity and diversity of PROTACs hinder the establishment of a clear structure–activity relationship²¹⁵. To address this issue, exploring the optimal linker characteristics for a specific biodegradation system could facilitate the rapid identification of more efficacious PROTACs. Secondly, the physico-chemical properties of the PROTACs often deviate from the classical “rule of five”¹⁹⁶, necessitating the investigation of drug-likeness rules tailored to PROTACs, to minimize the likelihood of designing PROTACs with poor pharmacokinetic profiles. Thirdly, purification and low yields, due to their large molecular weight and intricate structure, pose challenges in PROTAC synthesis and optimization³⁷. Therefore, the development of advanced synthetic techniques specific to PROTACs is essential to access a broader range of structural types. Finally, the large size of the ternary complex, consisting of POI-PROTAC-E3, can make crystal structure determination difficult²⁰⁶. To address this, the development of advanced crystallographic techniques or more accurate computational simulation methods is necessary to gain insights for further optimization. We believe that addressing these issues will significantly enhance the progress of PROTAC research. We anticipate that this study will prove to be an invaluable reference for further developments in the field of PROTAC.

Acknowledgments

This work was supported by the National Natural Science Foundation of China (No. 32125033, 32260688, China), Innovation and Entrepreneurship Project for Overseas Talents in Guizhou Province (No. [2022]03, China), Specific Natural Science Foundation of Guizhou University (No. [2022]42, China), and the Central Government Guides Local Science and Technology Development Fund Projects (Qiankehezhongyindi (2023) 001, China).

Author contributions

Yawen Dong conceived the idea and drafted the manuscript. Tingting Ma, Ting Xu, Zhangyan Feng, Yonggui Li, and Lingling Song contributed by creating representations of published PROTACs. Yawen Dong, Xiaojun Yao, Charles R. Ashby Jr., and Ge-Fei Hao reviewed and refined the manuscript meticulously before submission.

Conflicts of interest

The authors declare no conflicts of interest.

Appendix A. Supporting information

Supporting information to this article can be found online at <https://doi.org/10.1016/j.apsb.2024.04.007>.

References

- Chen Y, Tandon I, Heelan W, Wang Y, Tang W, Hu Q. Proteolysis-targeting chimera (PROTAC) delivery system: advancing protein degraders towards clinical translation. *Chem Soc Rev* 2022;51:5330–50.
- Chinnomaa D, Hornberger KR, Crews CM. Protein degraders enter the clinic—new approach to cancer therapy. *Nat Rev Clin Oncol* 2023;20:265–78.

3. Bekes M, Langley DR, Crews CM. PROTAC targeted protein degraders: the past is prologue. *Nat Rev Drug Discov* 2022;**21**: 181–200.
4. Li X, Song Y. Proteolysis-targeting chimera (PROTAC) for targeted protein degradation and cancer therapy. *J Hematol Oncol* 2020;**13**: 50.
5. Zhong L, Li Y, Xiong L, Wang W, Wu M, Yuan T, et al. Small molecules in targeted cancer therapy: advances, challenges, and future perspectives. *Signal Transduct Targeted Ther* 2021;**6**:201.
6. Zorba A, Nguyen C, Xu Y, Starr J, Borzilleri R, Smith J, et al. Delining the role of cooperativity in the design of potent PROTACs for BTK. *Proc Natl Acad Sci U S A* 2018;**115**: E7285–de7292.
7. Toure M, Crews C. Small-molecule PROTACs: new approaches to protein degradation. *Angew Chem Int Ed Engl* 2016;**55**:1966–73.
8. Sun X, Gao H, Yang Y, He M, Wu Y, Song Y, et al. PROTACs: great opportunities for academia and industry. *Signal Transduct Targeted Ther* 2019;**4**:64.
9. Ottis P, Crews CM. Proteolysis-targeting chimeras: induced protein degradation as a therapeutic strategy. *ACS Chem Biol* 2017;**12**:892–8.
10. Deshaies RJ. Protein degradation: prime time for PROTACs. *Nat Chem Biol* 2015;**11**:634–5.
11. Sun D, Zhang J, Dong G, He S, Sheng C. Blocking non-enzymatic functions by PROTAC-mediated targeted protein degradation. *J Med Chem* 2022;**65**:14276–88.
12. Lu M, Liu T, Jiao Q, Ji J, Tao M, Liu Y, et al. Discovery of a Keap1-dependent peptide PROTAC to knockdown Tau by ubiquitination-proteasome degradation pathway. *Eur J Med Chem* 2018;**146**:251–9.
13. Burslem GM, Song J, Chen X, Hines J, Crews CM. Enhancing antiproliferative activity and selectivity of a FLT-3 inhibitor by proteolysis targeting chimera conversion. *J Am Chem Soc* 2018;**140**: 16428–32.
14. Li X, Yao Y, Wu F, Song Y. A proteolysis-targeting chimera molecule selectively degrades ENL and inhibits malignant gene expression and tumor growth. *J Hematol Oncol* 2022;**15**:41.
15. Gu S, Cui D, Chen X, Xiong X, Zhao Y. PROTACs: an emerging targeting technique for protein degradation in drug discovery. *Bioessays* 2018;**40**:e1700247.
16. Chu TT, Gao N, Li QQ, Chen PG, Yang XF, Chen YX, et al. Specific knockdown of endogenous Tau protein by peptide-directed ubiquitin-proteasome degradation. *Cell Chem Biol* 2016;**23**:453–61.
17. Zhao L, Zhao J, Zhong K, Tong A, Jia D. Targeted protein degradation: mechanisms, strategies and application. *Signal Transduct Targeted Ther* 2022;**7**:113.
18. Cyrus K, Wehenkel M, Choi EY, Han HJ, Lee H, Swanson H, et al. Impact of linker length on the activity of PROTACs. *Mol Biosyst* 2011;**7**:359–64.
19. Lai AC, Toure M, Hellerschmied D, Salami J, Jaime-Figueroa S, Ko E, et al. Modular PROTAC design for the degradation of oncogenic BCR-ABL. *Angew Chem Int Ed Engl* 2016;**55**:807–10.
20. He S, Dong G, Cheng J, Wu Y, Sheng C. Strategies for designing proteolysis targeting chimaeras (PROTACs). *Med Res Rev* 2022;**42**: 1280–342.
21. Hines J, Lartigue S, Dong H, Qian Y, Crews CM. MDM2-recruiting PROTAC offers superior, synergistic antiproliferative activity via simultaneous degradation of BRD4 and stabilization of p53. *Cancer Res* 2019;**79**:251–62.
22. Bondeson DP, Smith BE, Burslem GM, Buhimschi AD, Hines J, Jaime-Figueroa S, et al. Lessons in PROTAC design from selective degradation with a promiscuous warhead. *Cell Chem Biol* 2018;**25**: 78–87.e5.
23. Bemis TA, La Clair JJ, Burkart MD. Unraveling the role of linker design in proteolysis targeting chimeras. *J Med Chem* 2021;**64**: 8042–52.
24. Wurz RP, Dellamaggiore K, Dou H, Javier N, Lo MC, McCarter JD, et al. A "click chemistry platform" for the rapid synthesis of bispecific molecules for inducing protein degradation. *J Med Chem* 2018; **61**:453–61.
25. Han X, Wang C, Qin C, Xiang W, Fernandez-Salas E, Yang CY, et al. Discovery of ARD-69 as a highly potent proteolysis targeting chimera (PROTAC) degrader of androgen receptor (AR) for the treatment of prostate cancer. *J Med Chem* 2019;**62**:941–64.
26. Farnaby W, Koegl M, Roy MJ, Whitworth C, Diers E, Trainor N, et al. BAF complex vulnerabilities in cancer demonstrated via structure-based PROTAC design. *Nat Chem Biol* 2019;**15**:672–80.
27. Zengerle M, Chan KH, Ciulli A. Selective small molecule induced degradation of the BET bromodomain protein BRD4. *ACS Chem Biol* 2015;**10**:1770–7.
28. Sakamoto KM, Kim KB, Kumagai A, Mercurio F, Crews CM, Deshaies RJ. Protacs: chimeric molecules that target proteins to the Skp1-Cullin-F box complex for ubiquitination and degradation. *Proc Natl Acad Sci U S A* 2001;**98**:8554–9.
29. Weerakoon D, Carbajo RJ, De Maria L, Tyrchan C, Zhao H. Impact of PROTAC linker plasticity on the solution conformations and dissociation of the ternary complex. *J Chem Inf Model* 2022;**62**: 340–9.
30. Schneekloth Jr JS, Fonseca FN, Koldobskiy M, Mandal A, Deshaies R, Sakamoto K, et al. Chemical genetic control of protein levels: selective *in vivo* targeted degradation. *J Am Chem Soc* 2004; **126**:3748–54.
31. Lee H, Puppala D, Choi EY, Swanson H, Kim KB. Targeted degradation of the aryl hydrocarbon receptor by the PROTAC approach: a useful chemical genetic tool. *Chembiochem* 2007;**8**: 2058–62.
32. Winter GE, Buckley DL, Pault J, Roberts JM, Souza A, Dhe-Paganon S, et al. Drug development. Phthalimide conjugation as a strategy for *in vivo* target protein degradation. *Science* 2015;**348**: 1376–81.
33. Raina K, Lu J, Qian Y, Altieri M, Gordon D, Rossi AM, et al. PROTAC-induced BET protein degradation as a therapy for castration-resistant prostate cancer. *Proc Natl Acad Sci U S A* 2016; **113**:7124–9.
34. Wu Y, Pu C, Fu Y, Dong G, Huang M, Sheng C, et al. NAMPT-targeting PROTAC promotes antitumor immunity via suppressing myeloid-derived suppressor cell expansion. *Acta Pharm Sin B* 2022; **12**:2859–68.
35. Henning RK, Varghese JO, Das S, Nag A, Tang G, Tang K, et al. Degradation of Akt using protein-catalyzed capture agents. *J Pept Sci* 2016;**22**:196–200.
36. Cross JM, Coulson ME, Smalley JP, Pytel WA, Ismail O, Trory JS, et al. A 'click' chemistry approach to novel entinostat (MS-275) based class I histone deacetylase proteolysis targeting chimeras. *RSC Med Chem* 2022;**13**:1634–9.
37. Lebraud HHT. Protein degradation: a validated therapeutic strategy with exciting prospects. *Essays Biochem* 2017;**61**:517–27.
38. Zhao Q, Lan T, Su S, Rao Y. Induction of apoptosis in MDA-MB-231 breast cancer cells by a PARP1-targeting PROTAC small molecule. *Chem Commun* 2019;**55**:369–72.
39. Zhu CL, Luo X, Tian T, Rao Z, Wang H, Zhou Z, et al. Structure-based rational design enables efficient discovery of a new selective and potent AKT PROTAC degrader. *Eur J Med Chem* 2022;**238**: 114459.
40. Tinworth CP, Lithgow H, Dittus L, Bassi ZI, Hughes SE, Muelbaier M, et al. PROTAC-mediated degradation of bruton's tyrosine kinase is inhibited by covalent binding. *ACS Chem Biol* 2019;**14**:342–7.
41. Jin YH, Lu MC, Wang Y, Shan WX, Wang XY, You QD, et al. AzoproTAC: novel light-controlled small-molecule tool for protein knockdown. *J Med Chem* 2020;**63**:4644–54.
42. Ko T, Jou C, Grau-Perales AB, Reynders M, Fenton AA, Trauner D. Photoactivated protein degrader for optical control of synaptic function. *ACS Chem Neurosci* 2023;**14**:3704–13.
43. Pfaff P, Samarasinghe KTG, Crews CM, Carreira EM. Reversible spatiotemporal control of induced protein degradation by bistable photoPROTACs. *ACS Cent Sci* 2019;**5**:1682–90.

44. Reynders M, Matsura BS, Bérouti M, Simoneschi D, Marzio A, Pagano M, et al. PHOTACs enable optical control of protein degradation. *Sci Adv* 2020;6:eaay5064.
45. Xue G, Wang K, Zhou D, Zhong H, Pan Z. Light-induced protein degradation with photocaged PROTACs. *J Am Chem Soc* 2019;141:18370–4.
46. Zhang Q, Kounde CS, Mondal M, Greenfield JL, Baker JR, Kotelnikov S, et al. Light-mediated multi-target protein degradation using arylazopyrazole photoswitchable PROTACs (AP-PROTACs). *Chem Commun* 2022;58:10933–6.
47. Schneekloth AR, Puchault M, Tae HS, Crews CM. Targeted intracellular protein degradation induced by a small molecule: en route to chemical proteomics. *Bioorg Med Chem Lett* 2008;18:5904–8.
48. Lebraud H, Wright DJ, Johnson CN, Heightman TD, Pye CR, Hewitt WM, et al. Protein degradation by in-cell self-assembly of proteolysis targeting chimeras. *ACS Cent Sci* 2016;2:927–34.
49. Bassi ZI, Fillmore MC, Miah AH, Chapman TD, Maller C, Roberts EJ, et al. Modulating PCAF/GCN5 immune cell function through a PROTAC approach. *ACS Chem Biol* 2018;13:2862–7.
50. Wu H, Yang K, Zhang Z, Leisten ED, Li Z, Xie H, et al. Development of multifunctional histone deacetylase 6 degraders with potent antimyeloma activity. *J Med Chem* 2019;62:7042–57.
51. Schiedel M, Herp D, Hammelmann S, Swyter S, Lehotzky A, Robaa D, et al. Chemically induced degradation of sirtuin 2 (Sirt2) by a proteolysis targeting chimera (PROTAC) based on sirtuin rearranging ligands (SirReals). *J Med Chem* 2018;61:482–91.
52. Bian J, Ren J, Li Y, Wang J, Xu X, Feng Y, et al. Discovery of Wogonin-based PROTACs against CDK9 and capable of achieving antitumor activity. *Bioorg Chem* 2018;81:373–81.
53. Sun Y, Zhao X, Ding N, Gao H, Wu Y, Yang Y, et al. PROTAC-induced BTK degradation as a novel therapy for mutated BTK C481S induced ibrutinib-resistant B-cell malignancies. *Cell Res* 2018;28:779–81.
54. Wu Y, Yang Y, Wang W, Sun D, Liang J, Zhu M, et al. PROTAC technology as a novel tool to identify the target of lathyrene diterpenoids. *Acta Pharm Sin B* 2022;12:4262–5.
55. Han X, Zhao L, Xiang W, Qin C, Miao B, Xu T, et al. Discovery of highly potent and efficient PROTAC degraders of androgen receptor (AR) by employing weak binding affinity VHL E3 ligase ligands. *J Med Chem* 2019;62:11218–31.
56. Degorce SL, Tavana O, Banks E, Crafter C, Gingipalli L, Kouchninov D, et al. Discovery of proteolysis-targeting chimera molecules that selectively degrade the IRAK3 pseudokinase. *J Med Chem* 2020;63:10460–73.
57. Zhao L, Han X, Lu J, McEachern D, Wang S. A highly potent PROTAC androgen receptor (AR) degrader ARD-61 effectively inhibits AR-positive breast cancer cell growth *in vitro* and tumor growth *in vivo*. *Neoplasia* 2020;22:522–32.
58. Takwale AD, Jo SH, Jeon YU, Kim HS, Shin CH, Lee HK, et al. Design and characterization of cereblon-mediated androgen receptor proteolysis-targeting chimeras. *Eur J Med Chem* 2020;208:112769.
59. Nunes J, McGonagle GA, Eden J, Kiritharan G, Touzet M, Lewell X, et al. Targeting IRAK4 for degradation with PROTACs. *ACS Med Chem Lett* 2019;10:1081–5.
60. Testa A, Hughes SJ, Lucas X, Wright JE, Ciulli A. Structure-based design of a macrocyclic PROTAC. *Angew Chem Int Ed Engl* 2020;59:1727–34.
61. Wang Y, Jiang X, Feng F, Liu W, Sun H, Cantrill C, et al. Degradation of proteins by PROTACs and other strategies. *Acta Pharm Sin B* 2020;10:207–38.
62. Structure-based design identifies PROTAC degraders of BAF complex subunits. *Cancer Discov* 2019;9:OF19.
63. Zaidman D, Prilusky J, London N. PRosettaC: Rosetta based modeling of PROTAC mediated ternary complexes. *J Chem Inf Model* 2020;60:4894–903.
64. Chen Q, Liu C, Wang W, Meng X, Cheng X, Li X, et al. Optimization of PROTAC ternary complex using DNA encoded library approach. *ACS Chem Biol* 2023;18:25–33.
65. Ma BH, Fan YZ, Zhang DZ, Wei Y, Jian YL, Liu DH, et al. *In silico* design of an androgen receptor DNA binding domain-targeted peptide PROTAC for prostate cancer therapy. *Adv Sci* 2022;9:e2201859.
66. Weng G, Cai X, Cao D, Du H, Shen C, Deng Y, et al. PROTAC-DB 2.0: an updated database of PROTACs. *Nucleic Acids Res* 2022;51:D1367–72.
67. Bondeson DP, Mares A, Smith IE, Ko E, Campos S, Miah AH, et al. Catalytic *in vivo* protein knockdown by small-molecule PROTACs. *Nat Chem Biol* 2015;11:611–7.
68. Gadd MS, Testa A, Lucas X, Chan KH, Chen W, Lamont DJ, et al. Structural basis of PROTAC cooperative recognition for selective protein degradation. *Nat Chem Biol* 2017;13:514–21.
69. Li L, Wu Y, Yang Z, Xu C, Zhao H, Liu J, et al. Discovery of KRAS G12C-IN-3 and pomalidomide-based PROTACs as degraders of endogenous KRAS G12C with potent anticancer activity. *Bioorg Chem* 2021;111:105447.
70. Cheng J, He S, Xu J, Huang M, Dong G, Sheng C. Making protein degradation visible: discovery of theranostic PROTACs for detecting and degrading NAMPT. *J Med Chem* 2022;65:15725–37.
71. Potjewyd F, Turner AW, Beri J, Rectenwald JM, Norris-Drouin JL, Cholensky SH, et al. Degradation of polycomb repressive complex 2 with an EED-targeted bivalent chemical degrader. *Cell Chem Biol* 2020;27:47–56.e15.
72. Wang Y, Zhou Y, Cao S, Sun Y, Dong Z, Li C, et al. *In vitro* and *in vivo* degradation of programmed cell death ligand 1 (PD-L1) by a proteolysis targeting chimera (PROTAC). *Bioorg Chem* 2021;111:104833.
73. Qiu X, Sun N, Kong Y, Li Y, Yang X, Jiang B, et al. Chemoselective synthesis of lenalidomide-based PROTAC library using alkylation reaction. *Org Lett* 2019;21:3838–41.
74. Zhao HY, Yang XY, Lei H, Xi XX, Lu SM, Zhang JJ, et al. Discovery of potent small molecule PROTACs targeting mutant EGFR. *Eur J Med Chem* 2020;208:112781.
75. McCoull W, Cheung T, Anderson E, Barton P, Burgess J, Byth K, et al. Development of a novel B-Cell lymphoma 6 (BCL6) PROTAC to provide insight into small molecule targeting of BCL6. *ACS Chem Biol* 2018;13:3131–41.
76. Khan S, Zhang X, Lv D, Zhang Q, He Y, Zhang P, et al. A selective BCL-X(L) PROTAC degrader achieves safe and potent antitumor activity. *Nat Med* 2019;25:1938–47.
77. Jiang Y, Deng Q, Zhao H, Xie M, Chen L, Yin F, et al. Development of stabilized peptide-based PROTACs against estrogen receptor alpha. *ACS Chem Biol* 2018;13:628–35.
78. He S, Fang Y, Wu M, Zhang P, Gao F, Hu H, et al. Enhanced tumor targeting and penetration of proteolysis-targeting chimeras through iRGD peptide conjugation: a strategy for precise protein degradation in breast cancer. *J Med Chem* 2023;66:16828–42.
79. Shi YY, Dong DR, Fan G, Dai MY, Liu M. A cyclic peptide-based PROTAC induces intracellular degradation of palmitoyltransferase and potently decreases PD-L1 expression in human cervical cancer cells. *Front Immunol* 2023;14:1237964.
80. Zhao Y, Shu Y, Lin J, Chen Z, Xie Q, Bao Y, et al. Discovery of novel BTK PROTACs for B-cell lymphomas. *Eur J Med Chem* 2021;225:113820.
81. Qi Z, Yang G, Deng T, Wang J, Zhou H, Popov SA, et al. Design and linkage optimization of ursane-thalidomide-based PROTACs and identification of their targeted-degradation properties to MDM2 protein. *Bioorg Chem* 2021;111:104901.
82. Kim GY, Song CW, Yang YS, Lee NR, Yoo HS, Son SH, et al. Chemical degradation of androgen receptor (AR) using bicalutamide analog-thalidomide PROTACs. *Molecules* 2021;26:2525.
83. Schiedel M, Lehotzky A, Szunyogh S, Oláh J, Hammelmann S, Wössner N, et al. HaloTag-targeted sirtuin-rearranging ligand (SirReal) for the development of proteolysis-targeting chimeras

- (PROTACs) against the lysine deacetylase sirtuin 2 (Sirt2). *Chem-biochem* 2020;21:3371–6.
84. Kang CH, Lee DH, Lee CO, Du HJ, Park CH, Hwang JY. Induced protein degradation of anaplastic lymphoma kinase (ALK) by proteolysis targeting chimera (PROTAC). *Biochem Biophys Res Commun* 2018;505:542–7.
 85. Lu J, Qian Y, Altieri M, Dong H, Wang J, Raina K, et al. Hijacking the E3 ubiquitin ligase cereblon to efficiently target BRD4. *Chem Biol* 2015;22:755–63.
 86. Cao Z, Gu Z, Lin S, Chen D, Wang J, Zhao Y, et al. Attenuation of NLRP3 inflammasome activation by indirubin-derived PROTAC targeting HDAC6. *ACS Chem Biol* 2021;16:2746–51.
 87. He Y, Zhang X, Chang J, Kim HN, Zhang P, Wang Y, et al. Using proteolysis-targeting chimera technology to reduce navitoclax platelet toxicity and improve its senolytic activity. *Nat Commun* 2020;11:1996.
 88. Salami J, Alabi S, Willard RR, Vitale NJ, Wang J, Dong H, et al. Androgen receptor degradation by the proteolysis-targeting chimera ARCC-4 outperforms enzalutamide in cellular models of prostate cancer drug resistance. *Commun Biol* 2018;1:100.
 89. Ambiard F, Cho JH, Schinazi RF. Cu(I)-catalyzed Huisgen azide-alkyne 1,3-dipolar cycloaddition reaction in nucleoside, nucleotide, and oligonucleotide chemistry. *Chem Rev* 2009;109:4207–20.
 90. Dong J, Miao J, Miao Y, Qu Z, Zhang S, Zhu P, et al. Small molecule degraders of protein tyrosine phosphatase 1B and T-cell protein tyrosine phosphatase for cancer immunotherapy. *Angew Chem Int Ed Engl* 2023;62:e202303818.
 91. Xia LW, Ba MY, Liu W, Cheng W, Hu CP, Zhao Q, et al. Triazol: a privileged scaffold for proteolysis targeting chimeras. *Future Med Chem* 2019;11:2919–73.
 92. Han X, Zhao L, Xiang W, Miao B, Qin C, Wang M, et al. Discovery of ARD-2051 as a potent and orally efficacious proteolysis targeting chimera (PROTAC) degrader of androgen receptor for the treatment of advanced prostate cancer. *J Med Chem* 2023;66:8822–43.
 93. Liu R, Liu Z, Chen M, Xing H, Zhang P, Zhang J. Cooperatively designed aptamer-PROTACs for spatioselective degradation of nucleocytoplasmic shuttling protein for enhanced combinational therapy. *Chem Sci* 2023;15:134–45.
 94. Tinworth CP, Lithgow H, Dittus L, Bassi ZI, Hughes SE, Muelbaier M, et al. PROTAC-mediated degradation of bruton's tyrosine kinase is inhibited by covalent binding. *ACS Chem Biol* 2019;14:342–7.
 95. Gockel LM, Pfeifer V, Baltes F, Bachmaier RD, Wagner KG, Bendas G, et al. Design, synthesis, and characterization of PROTACs targeting the androgen receptor in prostate and lung cancer models. *Arch Pharmazie* 2022;355:e2100467.
 96. Liu XG, Kalogeropoulou AF, Domingos S, Makukhin N, Nirujogi RS, Singh F, et al. Discovery of XL01126: a potent, fast, cooperative, selective, orally bioavailable, and blood–brain barrier penetrant PROTAC degrader of leucine-rich repeat kinase 2. *J Am Chem Soc* 2022;144:16930–52.
 97. Hamilton EP, Schott AF, Nanda R, Lu H, Keung CF, Gedrich R, et al. ARV-471, an estrogen receptor (ER) PROTAC degrader, combined with palbociclib in advanced ER+/human epidermal growth factor receptor 2-negative (HER2-) breast cancer: phase 1b cohort (part C) of a phase 1/2 study. *J Clin Oncol* 2022;40:TPS1120.
 98. Neklesa T, Snyder LB, Willard RR, Vitale N, Pizzano J, Gordon DA, et al. ARV-110: an oral androgen receptor PROTAC degrader for prostate cancer. *J Clin Oncol* 2019;37:259–259.
 99. Jackson KL, Agafonov RV, Carlson MW, Chaturvedi P, Cocozziello D, Cole K, et al. Abstract ND09: the discovery and characterization of CFT8634: a potent and selective degrader of BRD9 for the treatment of SMARCB1-perturbed cancers. *Cancer Res* 2022;82:ND09–ND09.
 100. Mayo M, Karnik R, Klaus C, Sharma K, McDonald A, Walker DH, et al. KT-413, a novel irakimide degrader of irak4 and imid substrates, has a differentiated MOA that leads to single-agent and combination regressions in myd88mt lymphoma models. *Hematol Oncol* 2021;39:37–8.
 101. Robbins DW, Kelly A, Tan M, McIntosh J, Wu J, Konst Z, et al. Nx-2127, a degrader of BTK and IMiD neosubstrates, for the treatment of B-Cell malignancies. *Blood* 2020;136:34.
 102. Niu T, Li K, Jiang L, Zhou Z, Hong J, Chen X, et al. Noncovalent CDK12/13 dual inhibitors-based PROTACs degrade CDK12–Cyclin K complex and induce synthetic lethality with PARP inhibitor. *Eur J Med Chem* 2022;228:114012.
 103. Zhang X, Thummuri D, He Y, Liu X, Zhang P, Zhou D, et al. Utilizing PROTAC technology to address the on-target platelet toxicity associated with inhibition of BCL-X(L). *Chem Commun* 2019;55:14765–8.
 104. Bollu LR, Bommi PV, Monsen PJ, Zhai L, Lauing KL, Bell A, et al. Identification and characterization of a novel indoleamine 2,3-dioxygenase 1 protein degrader for glioblastoma. *J Med Chem* 2022;65:15642–62.
 105. Hendrick CE, Jorgensen JR, Chaudhry C, Strambeanu II, Brazeau JF, Schiffer J, et al. Direct-to-biology accelerates PROTAC synthesis and the evaluation of linker effects on permeability and degradation. *ACS Med Chem Lett* 2022;13:1182–90.
 106. Li C, Qiao Y, Jiang X, Liu L, Zheng Y, Qiu Y, et al. Discovery of a first-in-class degrader for the lipid kinase PIKfyve. *J Med Chem* 2023;66:12432–45.
 107. Winter GE, Mayer A, Buckley DL, Erb MA, Roderick JE, Vittori S, et al. BET bromodomain proteins function as master transcription elongation factors independent of CDK9 recruitment. *Mol Cell* 2017;67:5–18.e9.
 108. Zhao N, Ho JSY, Meng F, Zheng S, Kurland AP, Tian L, et al. Generation of host-directed and virus-specific antivirals using targeted protein degradation promoted by small molecules and viral RNA mimics. *Cell Host Microbe* 2023;31:1154–1169.e10.
 109. Hung CL, Liu HH, Fu CW, Yeh HH, Hu TL, Kuo ZK, et al. Targeting androgen receptor and the variants by an orally bioavailable proteolysis targeting chimeras compound in castration resistant prostate cancer. *EBioMedicine* 2023;90:104500.
 110. Gunasekaran P, Hwang YS, Lee GH, Park J, Kim JG, La YK, et al. Degradation of polo-like kinase 1 by the novel poly-arginine n-degron pathway PROTAC regulates tumor growth in nonsmall cell lung cancer. *J Med Chem* 2024;67:3307–20.
 111. Zhou Z, Zhou G, Zhou C, Fan Z, Cui R, Li Y, et al. Discovery of a potent, cooperative, and selective SOS1 PROTAC ZZ151 with *in vivo* antitumor efficacy in KRAS-mutant cancers. *J Med Chem* 2023;66:4197–214.
 112. Gazorpak M, Hugentobler KM, Paul D, Germain PL, Kretschmer M, Ivanova I, et al. Harnessing PROTAC technology to combat stress hormone receptor activation. *Nat Commun* 2023;14:8177.
 113. Tseng YL, Lu PC, Lee CC, He RY, Huang YA, Tseng YC, et al. Degradation of neurodegenerative disease-associated TDP-43 aggregates and oligomers via a proteolysis-targeting chimera. *J Biomed Sci* 2023;30:27.
 114. Zeng S, Jin Y, Xia H, Shang Y, Li Y, Wang Z, et al. Discovery of highly efficient CRBN-recruiting HPK1-PROTAC as a potential chemical tool for investigation of scaffolding roles in TCR signaling. *Bioorg Chem* 2023;143:107016.
 115. Cromm PM, Samarasinghe KTG, Hines J, Crews CM. Addressing kinase-independent functions of Fak via PROTAC-mediated degradation. *J Am Chem Soc* 2018;140:17019–26.
 116. Yan G, Zhong X, Yue L, Pu C, Shan H, Lan S, et al. Discovery of a PROTAC targeting ALK with *in vivo* activity. *Eur J Med Chem* 2021;212:113150.
 117. Bagka M, Choi H, Heritier M, Schwaemmle H, Pasquer QTL, Braun SMG, et al. Targeted protein degradation reveals BET

- bromodomains as the cellular target of Hedgehog pathway inhibitor-1. *Nat Commun* 2023;14:3893.
118. Geiger TM, Walz M, Meyners C, Kuehn A, Dreizler JK, Sugiarto WO, et al. Discovery of a potent proteolysis targeting chimera enables targeting the scaffolding functions of FK506-binding protein 51 (FKBP51). *Angew Chem Int Ed Engl* 2024;63:e202309706.
 119. Yang H, Lv W, He M, Deng H, Li H, Wu W, et al. Plasticity in designing PROTACs for selective and potent degradation of HDAC6. *Chem Commun* 2019;55:14848–51.
 120. Gao H, Wu Y, Sun Y, Yang Y, Zhou G, Rao Y. Design, synthesis, and evaluation of highly potent FAK-targeting PROTACs. *ACS Med Chem Lett* 2020;11:1855–62.
 121. Donoghue C, Cubillos-Rojas M, Gutierrez-Prat N, Sanchez-Zarzalejo C, Verdaguer X, Riera A, et al. Optimal linker length for small molecule PROTACs that selectively target p38 α and p38 β for degradation. *Eur J Med Chem* 2020;201:112451.
 122. Naganuma M, Ohoka N, Tsuji G, Inoue T, Naito M, Demizu Y. Structural optimization of decoy oligonucleotide-based PROTAC that degrades the estrogen receptor. *Bioconjugate Chem* 2023;34:1780–8.
 123. Wang W, Liu Y, Xiong L, Sun D, Wang H, Song Z, et al. Synthesis of lathyrol PROTACs and evaluation of their anti-inflammatory activities. *J Nat Prod* 2023;86:767–81.
 124. Wang M, Lu J, Wang M, Yang CY, Wang S. Discovery of SHP2-D26 as a first, potent, and effective PROTAC degrader of SHP2 protein. *J Med Chem* 2020;63:7510–28.
 125. Wu T, Zhang Z, Gong G, Du Z, Xu Y, Yu S, et al. Discovery of novel flavonoid-based CDK9 degraders for prostate cancer treatment via a PROTAC strategy. *Eur J Med Chem* 2023;260:115774.
 126. Zhang B, Liu C, Yang Z, Zhang S, Hu X, Li B, et al. Discovery of BWA-522, a first-in-class and orally bioavailable PROTAC degrader of the androgen receptor targeting N-terminal domain for the treatment of prostate cancer. *J Med Chem* 2023;66:11158–86.
 127. Jarusiewicz JA, Yoshimura S, Mayasundari A, Actis M, Aggarwal A, McGowan K, et al. Phenyl dihydrouracil: an alternative cereblon binder for PROTAC design. *ACS Med Chem Lett* 2023;14:141–5.
 128. Mao W, Vandecan NM, Bingham CR, Tsang PK, Ulitz P, Sexton R, et al. Selective and potent PROTAC degraders of c-Src kinase. *ACS Chem Biol* 2024;19:110–6.
 129. Chen S, Chen Z, Lu L, Zhao Y, Zhou R, Xie Q, et al. Discovery of novel BTK PROTACs with improved metabolic stability via linker rigidification strategy. *Eur J Med Chem* 2023;255:115403.
 130. Sun Y, Xue Y, Sun P, Mu S, Liu H, Sun Y, et al. Discovery of the first potent, selective, and *in vivo* efficacious polo-like kinase 4 proteolysis targeting chimera degrader for the treatment of TRIM37-amplified breast cancer. *J Med Chem* 2023;66:8200–21.
 131. Xiang W, Zhao L, Han X, Xu T, Kregel S, Wang M, et al. Discovery of ARD-1676 as a highly potent and orally efficacious AR PROTAC degrader with a broad activity against AR mutants for the treatment of AR + human prostate cancer. *J Med Chem* 2023;66:13280–303.
 132. Chan K, Sathyamurthy PS, Queisser MA, Mullin M, Shrives H, Coe DM, et al. Antibody-proteolysis targeting chimera conjugate enables selective degradation of receptor-interacting serine/threonine-protein kinase 2 in HER2+ cell lines. *Bioconjugate Chem* 2023;34:2049–54.
 133. Sun Y, Yang Z, Zhang Z, Li Z, Guo L, Pan H, et al. Design, synthesis, and evaluation of BTK-targeting PROTACs with optimized bioavailability *in vitro* and *in vivo*. *RSC Med Chem* 2023;14:1562–6.
 134. Jin Y, Fan J, Wang R, Wang X, Li N, You Q, et al. Ligation to scavenging strategy enables on-demand termination of targeted protein degradation. *J Am Chem Soc* 2023;145:7218–29.
 135. Salami JA, Alabi S, Willard RR, Vitale NJ, Wang J, Dong H, et al. Androgen receptor degradation by the proteolysis-targeting chimera ARCC-4 outperforms enzalutamide in cellular models of prostate cancer drug resistance. *Commun Biol* 2018;1:100.
 136. Guo L, Liu J, Nie X, Wang T, Ma ZX, Yin D, et al. Development of selective FGFR1 degraders using a rapid synthesis of proteolysis targeting chimera (Rapid-TAC) platform. *Bioorg Med Chem Lett* 2022;75:128982.
 137. Kargo RB. Potent PROTACs targeting EGFR mutants in drug discovery. *ACS Med Chem Lett* 2022;13:1835–6.
 138. Alcock LJ, Chang Y, Jarusiewicz JA, Actis M, Nithianantham S, Mayasundari A, et al. Development of potent and selective janus kinase 2/3 directing PG-PROTACs. *ACS Med Chem Lett* 2022;13:475–82.
 139. Rathje OH, Perryman L, Payne RJ, Hamprecht DW. PROTACs targeting MLKL protect cells from necroptosis. *J Med Chem* 2023;66:11216–36.
 140. Yang L, Tu W, Huang L, Miao B, Kaneshige A, Jiang W, et al. Discovery of SMD-3040 as a potent and selective SMARCA2 PROTAC degrader with strong *in vivo* antitumor activity. *J Med Chem* 2023;66:10761–81.
 141. Chen Z, Hu BA-O, Rej RA-O, Wu D, Acharyya RK, Wang M, et al. Discovery of ERD-3111 as a potent and orally efficacious estrogen receptor PROTAC degrader with strong antitumor activity. *J Med Chem* 2023;66:12559–85.
 142. Guenette RGYS, Min J, Pei B, Potts PR. Target and tissue selectivity of PROTAC degraders. *Chem Soc Rev* 2022;51:5740–56.
 143. Zhang L, Li L, Wang X, Liu H, Zhang Y, Xie T, et al. Development of a novel PROTAC using the nucleic acid aptamer as a targeting ligand for tumor selective degradation of nucleolin. *Mol Ther Nucleic Acids* 2022;30:66–79.
 144. Xiao Z, Song S, Chen D, van Merkerk R, van Der Wouden PE, Cool RH, et al. Proteolysis targeting chimera (PROTAC) for macrophage migration inhibitory factor (MIF) has anti-proliferative activity in lung cancer cells degradation *in vivo*. *Angew Chem Int Ed* 2021;60:17514–21.
 145. Tonali N, Nencetti S, Orlandini E, Ciccone L. Application of PROTAC strategy to TTR-A β protein–protein interaction for the development of Alzheimer’s disease drugs. *Neural Regener Res* 2021;16:1554–5.
 146. Li W, Zhang J, Guo L, Wang Q. Importance of three-body problems and protein–protein interactions in proteolysis-targeting chimera modeling: insights from molecular dynamics simulations. *J Chem Inf Model* 2022;62:523–32.
 147. Smith BE, Wang SL, Jaime-Figueroa S, Harbin A, Wang J, Hamman BD, et al. Differential PROTAC substrate specificity dictated by orientation of recruited E3 ligase. *Nat Commun* 2019;10:131.
 148. Yang CY, Qin C, Bai L, Wang S. Small-molecule PROTAC degraders of the bromodomain and extra terminal (BET) proteins—review. *Drug Discov Today Technol* 2019;31:43–51.
 149. Bemis TALCJ, Burkart MD. Unraveling the role of linker design in proteolysis targeting chimeras. *J Med Chem* 2021;64:8042–52.
 150. Shao J, Yan Y, Ding D, Wang D, He Y, Pan Y, et al. Destruction of DNA-binding proteins by programmable oligonucleotide PROTAC (O’PROTAC): effective targeting of LEF1 and ERG. *Adv Sci* 2021;8:e2102555.
 151. Cao C, He M, Wang L, He Y, Rao Y. Chemistries of bifunctional PROTAC degraders. *Chem Soc Rev* 2022;51:7066–114.
 152. Lim S, Khoo R, Peh KM, Teo J, Chang SC, Ng S, et al. bioPROTACs as versatile modulators of intracellular therapeutic targets including proliferating cell nuclear antigen (PCNA). *Proc Natl Acad Sci U S A* 2020;117:5791–800.
 153. Wu J, Wang W, Leung CH. Computational strategies for PROTAC drug discovery. *Acta Materia Medica* 2023;2:42–53.
 154. Tang K, Jia Y, Yu B, Liu HM. Medicinal chemistry strategies for the development of protein tyrosine phosphatase SHP2 inhibitors and PROTAC degraders. *Eur J Med Chem* 2020;204:112657.
 155. Hu J, Hu B, Wang M, Xu F, Miao B, Yang CY, et al. Discovery of ERD-308 as a highly potent proteolysis targeting chimera (PROTAC) degrader of estrogen receptor (ER). *J Med Chem* 2019;62:1420–42.

156. Zhou Q, Wu W, Jia K, Qi G, Sun XS, Li P. Design and characterization of PROTAC degraders specific to protein N-terminal methylesterase 1. *Eur J Med Chem* 2022;244:114830.
157. Tang K, Wang B, Yu B, Liu HM. Indoleamine 2,3-dioxygenase 1 (IDO1) inhibitors and PROTAC-based degraders for cancer therapy. *Eur J Med Chem* 2022;227:113967.
158. Gao Y, Jiang B, Kim H, Berberich MJ, Che J, Donovan KA, et al. Catalytic degraders effectively address kinase site mutations in EML4-ALK oncogenic fusions. *J Med Chem* 2023;66:5524–35.
159. Iyer R, Jovanovska VP, Berginc K, Jaklić M, Fabiani F, Harlacher C, et al. Amorphous solid dispersions (ASDs): the influence of material properties, manufacturing processes and analytical technologies in drug product development. *Pharmaceutics* 2021;13:162.
160. Bala R, Sindhu RK, Madaan R, Yadav SK. PROTAC: a novel drug delivery technology for targeting proteins in cancer cells. *Curr Drug Discov Technol* 2023;20:63–73.
161. Liu M, Martyn AP, Quinn RJ. Natural product-based PROteolysis TArgeting chimeras (PROTACs). *Nat Prod Rep* 2022;39:2292–307.
162. Weng G, Li D, Kang Y, Hou T. Integrative modeling of PROTAC-mediated ternary complexes. *J Med Chem* 2021;64:16271–81.
163. Li B, Ran T, Chen H. 3D based generative PROTAC linker design with reinforcement learning. *Briefings Bioinf* 2023;24:bbad323.
164. Huang Y, Ma J, Zhang M. 3DLinker: an e(3) equivariant variational autoencoder for molecular linker design. *arXiv e-prints* 2022. arXiv: 2205.07309.
165. Imrie F, Bradley AR, van der Schaar M, Deane CM. Deep generative models for 3D linker design. *J Chem Inf Model* 2020;60:1983–95.
166. Tan Y, Dai L, Huang W, Guo Y, Zheng S, Lei J, et al. DRlinker: deep reinforcement learning for optimization in fragment linking design. *J Chem Inf Model* 2022;62:5907–17.
167. Jin J, Wang D, Shi G, Bao J, Wang J, Zhang H, et al. FFLOM: a flow-based autoregressive model for fragment-to-lead optimization. *J Med Chem* 2023;66:10808–23.
168. Guo J, Knuth F, Margreitter C, Janet JP, Papadopoulos K, Engkvist O, et al. Link-INVENT: generative linker design with reinforcement learning. *Digital Discov* 2023;2:392–408.
169. Neeser RM, Akdel M, Kovtun D, Naef L. Reinforcement learning-driven linker design via fast attention-based point cloud alignment. *arXiv e-prints* 2023. arXiv:2306.08166.
170. Kao CT, Lin CT, Chou CL, Lin CC. Fragment linker prediction using the deep encoder-decoder network for PROTACs drug design. *J Chem Inf Model* 2023;63:2918–27.
171. Danishuddin Jamal MS, Song KS, Lee KW, Kim JJ, Park YM. Revolutionizing drug targeting strategies: integrating artificial intelligence and structure-based methods in PROTAC development. *Pharmaceutics* 2023;16:1649.
172. Zheng S, Tan Y, Wang Z, Li C, Zhang Z, Sang X, et al. Accelerated rational PROTAC design via deep learning and molecular simulations. *Nat Mach Intell* 2022;4:739–48.
173. Li F, Hu Q, Zhang X, Sun R, Liu Z, Wu S, et al. DeepPROTACs is a deep learning-based targeted degradation predictor for PROTACs. *Nat Commun* 2022;13:7133.
174. Liu Z, Hu M, Yang Y, Du C, Zhou H, Liu C, et al. An overview of PROTACs: a promising drug discovery paradigm. *Mol Biomed* 2022;3:46.
175. Chardin P, Camonis JH, Gale NW, van Aelst L, Schlessinger J, Wigler MH, et al. Human Sos1: a guanine nucleotide exchange factor for Ras that binds to GRB2. *Science* 1993;260:1338–43.
176. Jeng HH, Taylor LJ, Bar-Sagi D. Sos-mediated cross-activation of wild-type Ras by oncogenic Ras is essential for tumorigenesis. *Nat Commun* 2012;3:1168.
177. Hofmann MH, Gmachi M, Ramharter J, Savarese F, Gerlach D, Marszalek JR, et al. BI-3406, a potent and selective SOS1-KRAS interaction inhibitor, is effective in KRAS-driven cancers through combined MEK inhibition. *Cancer Discov* 2021;11:142–57.
178. Frost J, Rocha S, Ciulli A. Von Hippel-Lindau (VHL) small-molecule inhibitor binding increases stability and intracellular levels of VHL protein. *J Biol Chem* 2021;297:100910.
179. Gmachi M, Sanderson M, Kessler D, Kofink C, Netherton MR, Ramharter J, et al. Novel benzylamino substituted quinazolines and derivatives as sos1 inhibitors. <https://pubchem.ncbi.nlm.nih.gov/patent/US-2019358230-A1> (accessed January 17, 2024).
180. Klein VG, Bond AG, Craigon C, Lokey RS, Ciulli A. Amide-to-ester substitution as a strategy for optimizing PROTAC permeability and cellular activity. *J Med Chem* 2021;64:18082–101.
181. Poongavanam V, Atilaw Y, Siegel S, Giese A, Lehmann L, Meibom D, et al. Linker-dependent folding rationalizes PROTAC cell permeability. *J Med Chem* 2022;65:13029–40.
182. Klein VG, Townsend CE, Testa A, Zengerle M, Maniaci C, Hughes SJ, et al. Understanding and improving the membrane permeability of VH032-based PROTACs. *ACS Med Chem Lett* 2020;11:1732–8.
183. Matsson P, Doak BC, Over B, Kihlberg J. Cell permeability beyond the rule of 5. *Adv Drug Deliv Rev* 2016;101:42–61.
184. Xiang TX, Anderson BD. The relationship between permeant size and permeability in lipid bilayer membranes. *J Membr Biol* 1994;140:111–22.
185. Pye CR, Hewitt WM, Schwochert J, Haddad TD, Townsend CE, Etienne L, et al. Nonclassical size dependence of permeation defines bounds for passive adsorption of large drug molecules. *J Med Chem* 2017;60:1665–72.
186. Doak BC, Over B, Giordanetto F, Kihlberg J. Oral druggable space beyond the rule of 5: insights from drugs and clinical candidates. *Chem Biol* 2014;21:1115–42.
187. Lipinski CA. Lead- and drug-like compounds: the rule-of-five revolution. *Drug Discov Today Technol* 2004;1:337–41.
188. Naylor MR, Ly AM, Handford MJ, Ramos DP, Pye CR, Furukawa A, et al. Lipophilic permeability efficiency reconciles the opposing roles of lipophilicity in membrane permeability and aqueous solubility. *J Med Chem* 2018;61:11169–82.
189. Gallenkamp D, Gelato KA, Haendler B, Weinmann H. Bromodomains and their pharmacological inhibitors. *ChemMedChem* 2014;9:438–64.
190. Belkina AC, Denis GV. BET domain co-regulators in obesity, inflammation and cancer. *Nat Rev Cancer* 2012;12:465–77.
191. Zuber J, Shi J, Wang E, Rappaport AR, Herrmann H, Sison EA, et al. RNAi screen identifies Brd4 as a therapeutic target in acute myeloid leukaemia. *Nature* 2011;478:524–8.
192. Baratta MG, Schinzel AC, Zwang Y, Bandopadhayay P, Bowman-Colin C, Kutt J, et al. An in-tumor genetic screen reveals that the BET bromodomain protein, BRD4, is a potential therapeutic target in ovarian carcinoma. *Proc Natl Acad Sci U S A* 2015;112:232–7.
193. Filippakopoulos P, Qi J, Picaud S, Shen Y, Smith WB, Fedorov O, et al. Selective inhibition of BET bromodomains. *Nature* 2010;468:1067–73.
194. Galdeano C, Gadd MS, Soares P, Scaffidi S, Van Molle I, Birced I, et al. Structure-guided design and optimization of small molecules targeting the protein–protein interaction between the von Hippel-Lindau (VHL) E3 ubiquitin ligase and the hypoxia inducible factor (HIF) alpha subunit with *in vitro* nanomolar affinities. *J Med Chem* 2014;57:8657–63.
195. Veber DF, Johnson SR, Cheng HY, Smith BR, Ward KW, Kopple KD. Molecular properties that influence the oral bioavailability of drug candidates. *J Med Chem* 2002;45:2615–23.
196. Edmondson SD, Yang B, Fallan C. Proteolysis targeting chimeras (PROTACs) in ‘beyond rule-of-five’ chemical space: recent progress and future challenges. *Bioorg Med Chem Lett* 2019;29:1555–64.
197. Young RJ, Green DV, Luscombe CN, Hill AP. Getting physical in drug discovery II: the impact of chromatographic hydrophobicity measurements and aromaticity. *Drug Discov Today* 2011;16:822–30.
198. Shultz MD. Two decades under the influence of the rule of five and the changing properties of approved oral drugs. *J Med Chem* 2019;62:1701–14.
199. Sung H, Ferlay J, Siegel RL, Laversanne M, Soerjomataram I, Jemal A, et al. Global cancer statistics 2020: globocan estimates of incidence and mortality worldwide for 36 cancers in 185 countries. *CA Cancer J Clin* 2021;71:209–49.

200. Jacob A, Raj R, Allison DB, Myint ZW. Androgen receptor signaling in prostate cancer and therapeutic strategies. *Cancers* 2021; **28**:5417.
201. Snyder L, Neklesa TK, Chen X, Dong H, Ferraro C, Gordon DA, et al. Abstract 43: discovery of ARV-110, a first in class androgen receptor degrading PROTAC for the treatment of men with metastatic castration resistant prostate cancer. *Cancer Res* 2021; **81**(13_Supplement):43.
202. Protein degradation therapeutics: PROTAC® drug discovery at Arvinas presented at 5th annual symposium on applied synthesis. Available from: <https://wwwarvinascom/wp-content/uploads/2023/05/Protein-Degradation-Therapeutics-PROTAC-Drug-Discovery-at-Arvinaspdf> (accessed January 15, 2024).
203. Hartmann MD, Boichenko I, Coles M, Zanini F, Lupas AN, Hernandez Alvarez B. Thalidomide mimics uridine binding to an aromatic cage in cereblon. *J Struct Biol* 2014; **188**:225–32.
204. Nique F, Hebbe S, Peixoto C, Annoot D, Lefrancois JM, Duval E, et al. Discovery of diarylyhdantoins as new selective androgen receptor modulators. *J Med Chem* 2012; **55**:8225–35.
205. Cyrus K, Wehenkel M, Choi EY, Lee H, Swanson H, Kim KB. Jostling for position: optimizing linker location in the design of estrogen receptor-targeting PROTACs. *ChemMedChem* 2010; **5**:979–85.
206. Zeng S, Huang W, Zheng X, Liyan C, Zhang Z, Wang J, et al. Proteolysis targeting chimera (PROTAC) in drug discovery paradigm: recent progress and future challenges. *Eur J Med Chem* 2021; **210**:112981.
207. Kim EK, Choi EJ. Pathological roles of MAPK signaling pathways in human diseases. *Biochim Biophys Acta, Mol Basis Dis* 2010; **1802**:396–405.
208. Cuadrado A, Nebreda AR. Mechanisms and functions of p38 MAPK signalling. *Biochem J* 2010; **429**:403–17.
209. Cargnello M, Roux PP. Activation and function of the MAPKs and their substrates, the MAPK-activated protein kinases. *Microbiol Mol Biol Rev* 2011; **75**:50–83.
210. Buckley DL, Raina K, Darricarrere N, Hines J, Gustafson JL, Smith IE, et al. HaloPROTACs: use of small molecule PROTACs to induce degradation of HaloTag fusion proteins. *ACS Chem Biol* 2015; **10**:1831–7.
211. Baumann A, Tuerck D, Prabhu S, Dickmann L, Sims J. Pharmacokinetics, metabolism and distribution of PEGs and PEGylated proteins: quo vadis?. *Drug Discov Today* 2014; **19**:1623–31.
212. Drummond ML, Williams CI. *In silico* modeling of PROTAC-mediated ternary complexes: validation and application. *J Chem Inf Model* 2019; **59**:1634–44.
213. Drummond ML, Henry A, Li H, Williams CI. Improved accuracy for modeling PROTAC-mediated ternary complex formation and targeted protein degradation via new *in silico* methodologies. *J Chem Inf Model* 2020; **60**:5234–54.
214. Gangwal RP, Das NR, Thanki K, Damre MV, Dhoke GV, Sharma SS, et al. Identification of p38 α MAP kinase inhibitors by pharmacophore based virtual screening. *J Mol Graph Model* 2014; **49**:18–24.
215. Luo G, Li Z, Lin X, Li X, Chen Y, Xi K, et al. Discovery of an orally active VHL-recruiting PROTAC that achieves robust HMGCR degradation and potent hypolipidemic activity *in vivo*. *Acta Pharm Sin B* 2021; **11**:1300–14.